Critical Assessment of the Performance of Density Functional Methods for Several Atomic and Molecular Properties

Kevin E. Riley[†], **Bryan T. Op't Holt**[†], and **Kenneth M. Merz Jr.**[‡]
Department of Chemistry and Quantum Theory Project, University of Florida, P.O. Box 118435, Gainesville, FL 32611-8435

Abstract

The reliable prediction of molecular properties is a vital task of computational chemistry. In recent years, density functional theory (DFT) has become a popular method for calculating molecular properties for a vast array of systems varying in size from small organic molecules to large biological compounds such as proteins. In this work we assess the ability of many DFT methods to accurately determine atomic and molecular properties for small molecules containing elements commonly found in proteins, DNA, and RNA. These properties include bond lengths, bond angles, ground state vibrational frequencies, electron affinities, ionization potentials, heats of formation, hydrogen bond interaction energies, conformational energies, and reaction barrier heights. Calculations are carried out with the 3-21G*, 6-31G*, 3-21+G*, 6-31+G*, 6-31++G*, cc-pVxZ, and aug-cc-pVxZ (x=D,T) basis sets, while bond distance and bond angle calculations are also done using the cc-pVQZ and aug-cc-pVQZ basis sets. Members of the popular functional classes, namely, LSDA, GGA, meta-GGA, hybrid-GGA, and hybrid-meta-GGA, are considered in this work. For the purpose of comparison, Hartree-Fock (HF) and second order many-body perturbation (MP2) methods are also assessed in terms of their ability to determine these physical properties. Ultimately, it is observed that the split valence bases of the 6-31G variety provide accuracies similar to those of the more computationally expensive Dunning type basis sets. Another conclusion from this survey is that the hybrid-meta-GGA functionals are typically among the most accurate functionals for all of the properties examined in this work.

1. Introduction

In the past several years it has become clear that, with the availability of increasingly powerful computers and improvements in computational methods, it will soon be possible to perform high-level *ab initio* calculations on large biological systems. Indeed, many DFT studies on biological systems have been carried out[1–25] and some preliminary large-scale biological studies, treating entire proteins, have already been performed using *ab initio* methods.[26–29] Density functional theory (DFT) methods scale favorably with molecular size compared to Hartree-Fock and post-Hartree-Fock methods and have the further advantage over the Hartree-Fock method of describing electron correlation effects.[30,31] For these reasons, DFT is the *ab initio* technique most well suited for studies on large compounds and promises to be at the forefront of *ab initio* investigations on biologically relevant systems such as proteins and DNA.

In this study, thirty-seven DFT methods along with HF and MP2 are assessed for their ability to accurately calculate nine molecular properties. These properties include bond lengths, bond angles, ground state vibrational frequencies, electron affinities (EA), ionization potentials (IP),

[‡]person to whom correspondence should be addressed; merz@qtp.ufl.edu.
[†]these authors contributed equally to this work

heats of formation (HOF), hydrogen bond interaction energies, conformational energies, and reaction barrier heights. Each property is associated with its own test set. For consistency, each density functional method, wave function method, and basis set considered in this survey was used to calculate each of the nine properties (except for EA for which non-diffuse basis functions were omitted).

DFT is not a single method, but a family of methods because the exact density functional is unknown. Density functional methods can be divided into several classes according to the types of functional dependencies that they possess; examples of the five commonly-used DFT categories are included in this study. The simplest type of DFT is the local spin density approximation (LSDA), which depends only on electron density. Generalized gradient approximation (GGA) functionals depend on the electron density and its reduced gradient, while meta-GGA functionals also depend on the kinetic energy density. Hybrid and meta-hybrid functionals are combinations of GGA and meta-GGA functionals with Hartree-Fock exchange. Table 1 lists all of the functionals investigated in this work and indicates the category to which each functional belongs. For the purpose of comparison to other popular molecular electronic structure methods, both the Hartree-Fock (HF) and second order many body perturbation (MP2) methods are also included in this study.

Perdew's "Jacob's ladder" approach for the systematic improvement of density functional approximations contains five rungs, with each possessing more accurate approximations than the one below it.[32] The five classes of density functionals investigated in this work contain elements of the first four rungs, with the hybrid-meta-GGA being the most complex. Functionals residing on the highest step in this scheme would include an exact exchange term and "exact partial correlation".[32,33] There have been a limited number of "fifth rung" functionals developed in the past few years, but these types of functionals are not yet widely used. An example of a "fifth rung" functional is that of Perdew and coworkers that combines exact exchange and second order correlation with a gradient-corrected density functional.[34,35] Since the use of functionals in this work is confined to more widely-used DFT methods, functionals from the fifth rung of "Jacob's ladder" are not included here.

In this study we employ a wide variety of basis sets ranging in size from the small, 3-21G*, basis to the very large, aug-cc-pVQZ, basis. The Pople type split valence basis sets, such as 3-21G, 6-31G, etc. are used extensively throughout chemistry and are very well validated, in this study we utilized five of these basis sets, namely, 3-21G*, 6-31G*, 3-21+G*, 6-31+G*, and 6-31++G*.[36–39] The correlation consistent basis sets of Dunning are also very widely used and are typically used in conjunction with high level, post-Hartree-Fock techniques such as the configuration interaction and coupled cluster methods.[40] These basis sets incorporate functions with high angular momentum (d,f,g,…) and have been optimized to describe correlation effects in atoms, but also describe correlation effects in molecules quite well.[41] It has been shown that, when used with DFT methods, the correlation consistent basis sets yield optimized geometries that agree with experiment very well. However, these basis sets have the disadvantage of being computationally expensive compared to the Pople type basis sets. In this work we employ the cc-pVxZ and aug-cc-pVxZ basis sets with x=D, T, and Q for geometry calculations, while all others are performed at the x=D, T levels. MP2 geometry optimization calculations at the cc-pVQZ and aug-cc-pVQZ levels are not performed because of their prohibitive cost. We realize that the most appropriate basis sets for each individual property may not have been included in our survey. However, after careful consideration, we decided to limit the number basis sets we employed due to computational constraints. We feel that the basis sets tested here are widely implemented and are familiar to most computational chemists.

This article contains a quantitative assessment of a wide variety of quantum chemical methods available in a widely used quantum chemistry software package. We have had to base our study

on a limited number of functionals and basis sets because of time considerations. New functionals are constantly being developed and it is impossible for a work such as this one to keep up with these new developments. Examples of more recent functionals are M05[42] and M05-2X[43] of Truhlar and co-workers, however these are not yet readily available for use. While we have included some analysis of the information garnered by this research, it is beyond the scope of these articles to discuss in depth the mathematical composition of functionals. Scuseria and Staroverov[44] have composed a review that provides an overview of the development of most classes of density functional methods. Readers interested in the development of these types of quantum methods should reference this and other similar reviews.

One of our primary interests is to predict the performance of density functional methods for calculations on biological systems. With this in mind, the test sets used in this work represent a collection of systems containing atoms commonly found in biomolecules such as proteins and DNA, namely C, H, N, O, S, and P. For most test sets, only systems whose physical properties have been determined experimentally have been included. All of the test sets employed in this survey are given in the supplemental material.

In order to estimate the performance of DFT methods in calculating accurate molecular geometries in proteins we have carried out geometry optimizations on a test set of 44 molecules whose structures are well characterized experimentally. The test set comprises 71 bond lengths and 34 bond angles that can be compared directly with experimental results. One would expect that the functional/basis set combination that is chosen to optimize these structures would have a great impact on the accuracy with which the bond lengths and angles can be computed, for this reason geometry optimizations have been carried out using a large number of density functional methods along with several basis sets. In a similar fashion, we have constructed a vibrational frequency test set of 35 molecules whose harmonic vibrational frequencies are experimentally well-characterized. A total of 145 vibrational frequencies are contained within this test set.

Several studies have been carried out to assess the performance of DFT methods for calculating molecular geometries and vibrational frequencies.[41,45–52] Johnson et al. conducted studies using the S (Slater), B (Becke88), SVWN5, BVWNV, SLYP, and BLYP functionals (as well as the HF, MP2, and QCISD methods) along with the 6-31G* basis set to asses the accuracy with which these methods predict bond lengths, bond angles, and vibrational frequencies, as well as atomic energies, dipole moments, and atomization energies.[52] For geometric and vibrational properties a test set composed of 32 small molecules from the G2 set was employed (44 bond lengths, 18 bond angles, and 110 frequencies). Raymond and Wheeler assessed the performance of the B3LYP method paired with the aug-cc-pVxZ (x=D,T,Q) basis sets in calculating the molecular geometries, energies, and harmonic vibrational frequencies of a set of 19 small inorganic molecules.[41] More recently, Wang and Wilson carried out studies using a test set of 17 molecules to determine the accuracy of molecular geometries and several other molecular properties calculated using the B3LYP, B3PW91, B3P86, BLYP, and BP86 functionals paired with the cc-pVxZ and aug-cc-pVxZ (x=D,T,Q,5) basis sets.[45] Riley et al. assessed the accuracy of the BLYP, B3LYP, SVWN5, c-SVWN5, and S (Slater) functionals, along with the 3-21G*, 3-21+G*, 6-311G**, and 6-311+G** basis sets, for calculating molecular geometries and vibrational frequencies along with several other atomic and molecular properties.[53]

Next, we consider three more physical properties: electron affinity, ionization potential, and heat of formation. The electron affinity is the energy gained by a neutral system upon attachment of an additional electron, thus forming an anion. This is a very challenging property to compute because of the difficulty associated with the treatment of anions and their, often

loosely bound, extra electron. The ionization potential, the energy required to remove an electron from a bound state to infinite separation, has been known for some time to be an important property of atoms and molecules. The ability to predict ionization potentials accurately has deep implications in the field of photoelectron spectroscopy. The heat of formation is the change in enthalpy that occurs when a molecule is formed from its constituent elements in their most stable states. This physical parameter is used to assess the stability of a molecule, to estimate the amount of energy released in a reaction, and to calculate other thermodynamic functions.[54]

The test sets used for the IP, EA, and HOF calculations are derived from the Gaussian G2/97 test set.[55,56] In an effort to increase the contribution of phosphorus-containing systems in our test sets, a few non-G2 additions have been made. The electron affinity test set contains 25 atoms and molecules, 24 of these come from the G2/97 test set while one of them, PO_2, does not. The ionization potential test set contains 37 atoms and molecules. All but one of these systems, PO_2, comes from the G2/97 test set. The heat of formation test set contains 156 molecules. Three of these molecules are not from the G2/97 set: PH, PO_2, and CH_3PH_2.

Several studies have been conducted to assess the performance of DFT and wave function-based methods in computing electron affinities, ionization potentials, and heats of formation.[54–63] Curtiss *et al* carried out a study to evaluate density functional methods as well as the Gaussian-2 method for computing electron affinities and ionization potentials using a test set including 58 electron affinities and 88 ionization potentials.[56] In this study the B3LYP, B3PW91, B3P86, BLYP, BP86, and SVWN functionals were used along with the 6-311+G (3*df*,2*p*) basis set. Ernzerhof and Scuseria evaluate the performance of the SVWN, SVWN5, BLYP, B3LYP, VSXC, PBEPBE, and PBE1PBE functionals for calculating atomization energies, ionization potentials, electron affinities, and bond lengths, this study was also carried out using the 6-311+G(3*df*,2*p*) basis set.[63] Curtiss *et al* assess the SVWN, BLYP, and B3LYP methods along with several Gaussian-3 methods for calculation of heats of formation, ionization potentials, electron affinities, and proton affinities using the 6-311+G(3*df*,2*p*) basis set.[57] Brothers and Merz carried out a study in which several LSDA, GGA, and hybrid-GGA functionals were evaluated for the computation of heats of formation with small basis sets, namely 3-21G*, 3-21+G*, and MIDI!.[61]

Another goal of this work is to assess the performance of DFT for describing hydrogen bonding interaction energies, conformational energies, and reaction barrier heights. Hydrogen bonding plays a critical role in many physical phenomena, among other things, these interactions are important in the formation of clusters, the stability of large molecules such as proteins, DNA, and polysaccharides, and in the formation of protein ligand complexes. Conformational energies are an important measure of a computational method's ability to accurately predict both the geometry and the electronic energy of a molecular system. The reaction barrier height is a measure of the energy necessary to drive a stable system into a metastable transition state; this property has important implications in chemical reactions and kinetics.

The hydrogen bonding test set contains ten hydrogen bound systems whose interaction energies have been well characterized by high-level theoretical techniques. The conformational energy test comprises ten small molecules whose experimental conformational energies are known. There are two different barrier height test sets, the first of these contains 23 barrier heights for hydrogen transfer reactions of small molecules with radical (non-singlet) transition states, while the second contains six barrier heights for reactions of larger molecules with singlet transition states. Henceforth in this work the former of these test sets will be referred to as the small radical barrier height set (SRBH) and the latter will be referred to as the large singlet barrier height set (LSBH).

Several studies have been carried out to assess the accuracy of density functional theory in predicting hydrogen bonding interaction energies.[64–73] Tsuzuki and Lüthi evaluated the BLYP, B3LYP, and PW91PW91 functionals, as well as the MP2 and HF methods, for the prediction of hydrogen bond interaction energies. These studies were carried out using the Dunning type basis sets, cc-pVxZ (x=D, T, Q, 5). Zhao and Truhlar carried out studies to determine the accuracy of DFT methods for several types of non-bonding interactions. These are hydrogen bonding, charge transfer, dipole interaction, and the weak (dispersion) interaction. These studies were done using a very large number of functionals along with the 6-31+G(*d,p*), MG3S[74] (a modified version of 6-31+G(*3d2f, 2df,2p*), and aug-cc-pVTZ basis sets. To our knowledge, there have been only a limited number of studies concerned with the accuracy with which DFT methods predict conformational energies.[74–76] Lynch, Zhao, and Truhlar evaluate the conformational energies of several conformer pairs of 1,2-ethandiol and butadiene. These studies were done using a number of functionals based on the MPW correlation functional along with several basis sets. There have been a number of studies carried out to evaluate the accuracy with which DFT methods describe reaction barrier heights.[77–81] In a recent study, Zhao, Gonzáles-García, and Truhlar test the accuracy of a large number of functionals along with several different basis sets for calculating the barrier heights of 38 hydrogen transfer and 38 non-hydrogen transfer reactions.[78]

2. Methods

All of the calculations carried out in this study were performed using Gaussian 03 version C. 01.[82] The authors were informed that MPWKCIS, MPW1KCIS, PBEKCIS, and PBE1KCIS functionals were not correctly coded in Gaussian 03 ver. C.01. Therefore, calculations involving these functionals were re-run using Gaussian 03 ver. D.01. For DFT calculations, the default numerical grid in Gaussian 03 was used to evaluate the density functional theory integrals. Geometry optimizations were carried out for each of the functional/basis set combinations using the default optimization algorithm in Gaussian 03.

Previous studies have used molecular geometries obtained at high levels of theory for the calculation of molecular properties at lower levels of theory. Because information based on high levels of theory is not available for large biomolecules, we feel that it is more appropriate to optimize the molecular geometry using the same basis set and density functional that is being evaluated for some given molecular property. In this work, most physical properties are evaluated at the geometric minimum obtained using the same method/basis set combination. Unfortunately, because of computer time-restrictions, it was not possible to optimize the molecules from the heat of formation test-set at the aug-cc-pVTZ level. For these calculations, single point calculations at theTPSS1KCIS/aug-cc-pVDZ optimized geometry, were used to estimate the heat of-formation.

Ionization potentials and electron affinities were calculated adiabatically. Only basis sets containing diffuse functions were considered for electron affinity calculations. This was done because is it well known that diffuse functions are necessary in order to properly treat anions. Heats of formation were calculated using the method specified in "Thermochemistry in Gaussian" white paper available at http://www.Gaussian-.com/g_whitepap/thermo.htm.[83] Values for ionization potentials and electron affinities were calculated adiabatically. Most experimental data for heats of formation, ionization potentials, and electron affinities were obtained from the G2/97 and G3 test set papers, additional experimental data for phosphorus compounds were obtained from the NIST chemistry WebBook at http://www.nist.gov.[84]

For the investigations involving the small radical barrier height test set, because of substantial problems associated with transition state convergence, we have used the geometries determined

by Lynch and Truhlar at the QCISD/MG3 level for all calculations of this property (see http://comp.chem.umn.edu/truhlar/).[77]

For the hydrogen bonding interaction energy calculations the counterpoise method of Boys and Bernardi is employed in order to account for the basis set superposition error.[85] For each level of theory considered in this work the geometries of the hydrogen bound dimers are fully optimized on the counterpoise hypersurface, the constituent monomers are also fully optimized. Because of the difficulties associated with the extraction of the zero-point-exclusive binding energies from experimental data, we have used binding energies obtained at a very high level of theory as reference values. These reference values were determined at the CCSD(T) basis set limit by Tsuzuki and Lüthi.[72]

Experimental conformational energy reference data were all obtained from reference [86]. These quantities are calculated as potential energy differences, that is, the difference in electronic energy between the most stable conformer and the least stable one. This is the method employed in several other studies.[87–89]

The barrier height reference data for the test set of small radical reactions (SBH) are in the form of zero point exclusive, Born-Oppenheimer, barrier heights. These barrier heights are simply calculated as the difference in electronic energy between the transition state and the reactants. For the large singlet test set (LSBH), the data are all directly from experiment and so it is necessary to include vibrational effects into the calculation of the barrier heights. These barrier heights are calculated as the difference in the thermally corrected total enthalpy between the transition state and the ground state of the reactant(s). For all six reactions in the singlet set, initial coordinates of the transition states were constructed to have sensible transition state-like geometries. The transition state optimization method in Gaussian 03 was implemented using the *ts*, *calcall*, and *noeigentest* keywords. Reaction barrier heights were obtained from optimized reactant and transition state structures for all functional and basis set combinations. MP2/aug-ccpVDZ and MP2/aug-cc-pVTZ LSBH reaction calculations were not performed due to their considerable computational expense.

3. Discussion

3.1 Bond Lengths

The average unsigned bond length errors for the gradient corrected, GGA, hybrid-GGA, meta-GGA, and hybrid-meta-GGA functionals, with Pople type basis sets are given in Figure 1. HF, MP2, and LSDA results are given in Table 2. Inspection of these figures reveals that the hybrid-GGA and hybrid-meta-GGA methods generally yield the lowest bond length errors when paired with these basis sets. The GGA and meta-GGA functionals both yield similar results with errors that are slightly greater than those of the hybrid and hybrid-meta functionals. Among the LSDA functionals, SVWN5 and SPL obtain errors that are comparable to those of GGA and meta-GGA while c-SVWN5 yields errors that are higher than the other LSDA methods. Of the GGA functionals, from the meta-GGA class, the VSXC functional yields the lowest unsigned bond length errors.

Figure 2 gives average unsigned bond length errors for the gradient corrected methods along with the Dunning type basis sets. It can be seen that, overall, the hybrid-GGA functionals yield the lowest errors. Meta-GGA functionals and hybrid-meta-GGA functionals perform nearly as well, followed by the GGA functionals. LSDA methods yield errors that are generally higher than those of GGA functionals. It should be noted that, for the smallest of the Dunning type basis sets, cc-pVDZ and aug-cc-pVDZ, the hybrid-GGA and hybrid-meta-GGA methods generally outperform all other methods by a significant margin. For the larger, cc-pVTZ, cc-pVQZ, aug-cc-pVTZ, and aug-cc-pVQZ, basis sets the hybrid-GGA, hybrid-meta-GGA, and

meta-GGA functionals all yield, on average, comparable results. As in the case of the Pople type basis sets, VSXC yields the lowest bond length errors.

Generally, increasing the basis set size results in smaller bond length errors, the most dramatic improvements can be seen when the small 3-21G* and 3-21+G* basis sets are compared to the 6-31G* and 6-31+G* basis sets. The addition of diffuse functions to hydrogen atoms in the 6-31++G* makes little difference in the magnitudes of bond length errors. For the Dunning type bases, the addition of diffuse functions improves accuracy only slightly. It is interesting to note that for all of the functionals considered here, the bond length errors obtained using the 6-31G* and 6-31+G* basis sets are lower than those obtained using the much more computationally expensive cc-pVDZ and aug-ccpVDZ basis sets.

One of key feature of the bond length data is that, there is little variation within a particular functional class for a given basis set. For example, the average unsigned bond length errors calculated with the hybrid-GGA functionals along with the 6-31G* basis set are all within 0.002Å of one another. This trend is especially evident for the GGA, hybrid-GGA, and meta-GGA functionals whereas there is quite a bit more variation within the LSDA and hybrid-meta-GGA class of functionals. Another aspect of this trend is that, typically, the amount of variation within a particular functional class decreases as the basis set size increases. Individual functionals that deviate significantly from the other functionals within their class are c-SVWN, HCTH, B98, VSXC, and BB1K.

For singlets, the hybrid-GGA and hybrid-meta-GGA methods yield the lowest errors when paired with most basis sets. However, for the TZ bases hybrid-GGA, meta-GGA, and hybrid-meta-GGA methods yield the best singlet results. For the small Pople type basis sets, 3-21G* and 3-21+G* the LSDA methods yield results that are slightly better than those of the GGA functionals. At higher basis sets, the all other density functional classes outperform the LSDA methods. In terms of radical systems, the hybrid-GGA and hybrid-meta-GGA are the density functional methods that yield the lowest bond length errors for all basis sets, since the best results overall are obtained by MP2. For all basis sets, the meta-GGA methods obtain errors that are higher than those of the hybrid-GGA and hybrid-meta-GGA methods.

For all methods except MP2, single and triple bonds are calculated much more accurately than double bonds. For all basis sets the LSDA, GGA, and meta-GGA methods tend to yield lower unsigned errors for triple bonds than for double bonds. Hybrid-GGA and hybrid-meta-GGA also obtain lower errors for triple bonds (compared to single bonds) when paired with Pople type and cc-pVDZ/aug-cc-pVDZ basis sets, but give higher errors for triple bonds with the larger Dunning type basis sets. Hartree-Fock and MP2 generally obtain lower bond length errors for single bonds than triple bonds.

3.2 Bond Angles

The average unsigned bond angle errors are shown in Figure 3 and Figure 4 and in Table 2. Generally, the hybrid-GGA and hybrid-meta-GGA methods produce the lowest errors. The best results among the small basis sets are generally obtained with the hybrid-GGA functionals along with the 3-21G* basis set. The hybrid-meta-GGA functionals also yield very good results although there is some of variation within this class. The LSDA methods produce bond angle errors that are higher than most of the gradient corrected functionals. The addition of diffuse functions to the basis set results in a significant increase in the average bond angle errors for these functionals. The SVWN5 and SPL functionals both yield very similar errors while the c-SVWN5 functional obtains results that are only slightly better than its LSDA counterparts when paired with the small bases. Overall, the best small basis set results are obtained by the B1LYP/3-21G* and PBE1PBE/3-21G* methods which both calculate the average unsigned bond angle error to be 1.36°.

The larger Pople basis sets, 6-31G*, 6-31+G*, and 6-31++G*, generally produce better bond angle results for the basis sets containing diffuse functions. The wave function based methods yield lower errors when paired with the 6-31G* basis set. It should also be noted that the addition of diffuse functions to hydrogen atoms in the 6-31++G* basis set does not result in any significant improvement over the 6-31+G* basis. Once again, the hybrid-GGA and hybrid-meta-GGA methods generally give the lowest unsigned bond angle errors. As in the case of the small Pople basis sets, there is a great deal of variation in the meta-GGA class of functionals. LSDA methods all yield similar results when paired with basis sets containing diffuse functions. However, the c-SVWN5 functional produces errors that are significantly higher than those of SVWN5 and SPL when paired with the 6-31G* basis set. For 6-31G*, HF generally outperforms the GGA and meta-GGA methods and yields errors that are higher than those of all hybrid-GGA and hybrid-meta-GGA methods.

One aspect of the data for the Dunning type basis sets is that the errors obtained with the cc-pVDZ basis set are much higher than those of all other Dunning basis sets for all methods considered except Hartree-Fock. In fact, cc-pVDZ is generally outperformed by all other basis sets, with the exception of 3-21+G*, for all functional methods. The hybrid-GGA and hybrid-meta-GGA functionals generally yield the lowest unsigned bond angle errors for the Dunning type basis sets. Generally speaking, increasing the basis set size results in lower unsigned errors, this trend is especially evident for the GGA and meta-GGA functionals paired with non-diffuse basis sets. When diffuse functions are added to the cc-pVTZ basis set there is a significant increase of accuracy for GGA and meta-GGA functionals. For most functionals there is a small decrease in bond angle error upon addition of diffuse functions to cc-pVQZ. Overall, the lowest error of $1.11°$ is obtained by the hybrid-GGA PBE1PBE/aug-cc-pVQZ method. PBEP86 and MPWP86 are the GGA functionals that typically yield the lowest unsigned bond angle errors, while HCTH is the least accurate in this class. It should be noted that BLYP exhibits trends that are quite different than those of other GGA functionals. BLYP/aug-cc-pVDZ yields errors that are much higher than all other GGA/aug-cc-pVDZ combinations while BLYP/aug-cc-pVTZ produces errors that are significantly lower than all other GGA/augcc-pVTZ combinations. LSDA methods all yield similar results with the exception of c-SVWN/cc-pVDZ. HF performs better when paired with the non-diffuse basis sets and larger Dunning-type bases generally yield larger errors than the smaller Dunning bases. The unsigned bond angle errors obtained with MP2 improve with increasing basis set size and with the addition of diffuse functions to the basis set.

HF, MP2, LSDA, GGA, and meta-GGA methods obtain lower bond angle errors for singlet states for most Dunning and large Pople type basis sets. By and large, the hybrid-GGA and hybrid-meta-GGA methods yield lower errors for radicals than for singlets. Most methods produce better results for radical species when paired with the 3-21+G* basis set. For singlets, the LSDA functionals produce the lowest unsigned bond angle errors among all functional based methods when paired with the Dunning type basis sets except cc-pVDZ and with the 6-31+G* and 6-31++G* Pople type basis sets. Hybrid-GGA methods give the lowest errors among DFT methods for 3-21G* and 6-31G*. In terms of radical species, the hybrid-GGA methods give the lowest unsigned bond angle errors for all basis sets considered in this work. Hybrid-meta-GGA methods generally produce errors that are slightly larger than those of hybrid-GGA functionals.

3.3 Vibrational Frequencies

Figure 5 and Figure 6 show the average unsigned vibrational frequency errors for gradient corrected DFT methods. Vibrational errors for the LSDA methods as well as HF and MP2 are given in Table 2. It has been observed previously that frequency errors for MP2 and HF methods are larger than those of most DFT methods. It is observed in this study that the hybrid-GGA

and hybrid-meta-GGA functionals, which include a Hartree-Fock like exchange term, are less accurate than other classes of DFT functionals in predicting harmonic vibrational frequencies. As expected, HF and MP2 errors are far worse than errors obtained with DFT calculations. Compared with the GGA, meta-GGA, and LSDA classes of functionals, MP2 errors are higher by a factor of about two or three, while HF errors are typically about three to five times higher. The lowest vibrational frequency error obtained by the MP2 method is 113 cm^{-1} for MP2/aug-cc-pVDZ while its highest error is 151 cm^{-1} for MP2/3-21G*. HF errors for vibrational frequencies range from 203 cm^{-1}, for HF/3-21+G*, to 236 cm^{-1}, for HF/6-31G*.

The inclusion of diffuse functions in the basis set does not greatly affect the ability of the functionals to predict vibrational frequencies. As shown in the figures, 3-21G* and 3-21+G* are nearly identical in performance. There is only a small improvement, on the order of 5 cm^{-1}, with the use of the 6-31+G* and 6-31++G* basis sets as opposed to 6-31G*. Augmented correlation-consistent basis sets do not perform markedly better than their non-diffuse counterparts for the double-zeta and triple-zeta basis sets.

The three LSDA functionals yield lower average errors than hybrid-meta-GGA and hybrid-GGA functionals, but they are generally higher than the errors of meta-GGA and GGA functionals. The SPL and SVWN5 functionals perform slightly better than c-SVWN5, with SPL performing the best of the three. The 6-31+G* and 6-31++G* basis sets yield the lowest errors for the SPL functional, around 50 cm-1.

Within the GGA class, there is little variation of performance between functionals with the exception of HCTH, which yields vibrational frequency errors that are significantly higher than any of the other functionals. In this class the Dunning style triple-zeta basis sets give the lowest unsigned vibrational frequency errors. Both the diffuse and non-diffuse variants of this basis set produce unsigned errors of 40-44cm^{-1}. It is interesting to note that the 6-31+G* and 6-31++G* basis sets, which are much less computationally expensive than the cc-pVTZ and aug-cc-pVTZ basis sets, yield errors that are only 5-8 cm^{-1} higher than these Dunning type basis sets. 6-31+G* and 6-31++G* also give results that typically outperform the cc-pVDZ and aug-cc-pVTZ basis sets. Of the 16 functionals in the GGA family, we find that MPWLYP and MPWP86 perform the best, but their advantage over most of the other functionals is only slight.

B3LYP is the most accurate of the hybrid-GGA class for calculating vibrational frequencies. B3LYP/cc-pVDZ yields the lowest error in this class at 70 cm^{-1}. PBE1PBE does not perform as well as the other members of this class. The meta-GGA class also shows some variance between functionals. VSXC, which is among the best meta-GGA methods for calculating bond lengths, performs poorly for vibrational frequencies. BB95, MPWB95, MPWKCIS and PBEKCIS are similar in performance throughout. BB95/augcc-pVTZ and MPWB95/aug-cc-pVTZ yield the lowest error of the class at 43 cm^{-1}. Finally, the hybrid-meta-GGA group does not perform as well as most other classes due to its inclusion of the HF exchange. TPSS1KCIS and MPW1KCIS are the best functionals in this functional class, the cc-pVTZ and aug-cc-pVTZ basis sets typically give the lowest average errors within this group.

3.4 Electron Affinities

The electron affinity average unsigned errors are shown in Table 3 and in Figure 7, the first of these gives the results for the HF, MP2, B3P86, and LSDA functional methods, the second gives all GGA, hybrid-GGA, meta-GGA, and hybrid-meta-GGA functional method results except for the hybrid-GGA functional B3P86, which yields very poor results. The best overall result for electron affinities is obtained using the meta-GGA functional MPWB95 along with the 6-31++G* basis set yielding an average unsigned error of 3.08 kcal/mol. The worst average unsigned error among the DFT methods is 16.78 kcal/mol and is obtained with the hybrid-GGA B3P86 functional combined with the 3-21+G* basis set. Among all methods studied in

this work, the HF/aug-cc-pVTZ method yields the worst result with an average error of 29.63 kcal/mol.

Among all of the functional types considered here, the LSDA methods produce the highest errors, this is an expected result as these are the least sophisticated functionals and the y lack gradient dependent terms. It is also interesting to note that results obtained with methods that incorporate the P86 correlation functional, with the exception of G96P86, are significantly worse than those obtained using the other functionals within a given class.

Of the three LSDA functionals the best result of 6.25 kcal/mol is obtained with SVWN5/6-31 +G*. Among the GGA functionals the PW91LYP/6-31++G* method yields the lowest average unsigned error of 3.56 kcal/mol, the PW91LYP/6-31+G*, PBEPW91/6-31++G*, and PBELYP/6-31++G* functional/basis set combinations all obtain errors lower than 3.60 kcal/mol. The B98/aug-cc-pVTZ method gives the smallest average error among the hybrid-GGA functionals of 3.15 kcal/mol. Among the meta-GGA functionals, the MPWB95/6-31++G* method yields the lowest error with a value of 3.08 kcal/mol, it is also noteworthy that the MPWB95/6-31+G* functional gives extremely good results with an error value of 3.12 kcal/mol. The MPW1KCIS/aug-cc-pVTZ method yields an error value of 3.48 kcal/mol, the lowest error among all hybrid-meta-GGA methods.

The Hartree-Fock method performs very poorly in describing electron affinities. This can be explained by the fact that, since an anion has one electron more than its neutral counterpart, correlation effects have a stronger effect on the negatively charged ion than on the neutral system. Due to the neglect of correlation effects in the Hartree-Fock technique, there is a pronounced discrepancy in its description of neutral and anionic species.

One salient aspect of these data is that, not surprisingly, the 3-21+G* basis set performs very poorly compared to the larger basis sets for all functionals. This basis set does, however, outperform all other basis sets when combined with the Hartree-Fock method and gives results that are only slightly worse than those obtained with the larger, 6-31+G* and 6-31++G*, basis sets when combined with the MP2 method. The lowest unsigned error for the very small (and inexpensive) 3-21+G* basis set is 5.17 kcal/mol as calculated with the BB95 functional.

It is also surprising that, generally, the 6-31+G* and 6-31++G* basis sets obtain results that are comparable to, or in many cases superior to, the aug-cc-pVDZ and aug-cc-pVTZ results. As can be seen in Figure 7 and Table 3, the average unsigned errors for the 6-31+G* and 6-31++G* basis sets are generally lower than those for the aug-cc-pVDZ and aug-cc-pVTZ basis sets for the LSDA, GGA, and meta-GGA functional classes. This trend is especially pronounced for the LSDA and GGA functionals, two of the three LSDA functionals obtain better results when combined with the smaller, Pople 6-31G type, basis sets compared to the results they obtained when used in conjunction with the larger, Dunning cc-pVXZ type, basis sets. The Pople type basis sets outperform the Dunning type basis sets for thirteen of the sixteen GGA functionals. For the hybrid-GGA and hybrid-meta-GGA functionals the Dunning type basis sets typically outperform the Pople type basis sets by a small margin (≤0.5kcal/mol). The meta-GGA functionals represent a "mixed bag" in terms of this trend, here the smaller basis sets outperform the larger ones (not including the 3-21+G* basis set) for four of the seven functionals studied in this work.

It should be noted that the addition of diffuse functions to hydrogen atoms in the 6-31++G* basis set does not lead to results that are significantly different than those obtained with the 6-31+G* basis set. It is also interesting to note that the aug-cc-pVTZ basis set generally yields results that are only slightly better than the aug-cc-pVDZ basis set results.

3.5 Ionization Potentials

The average ionization potential unsigned errors for each functional/basis set combination are given in Figure 8 and Figure 9 and in Table 3. Table 3 gives results of HF, MP2, LSDA functionals, and B3P86 (which yields high errors) for all basis sets. The best result for ionization potentials is obtained with the hybrid-meta-GGA functional B1B95 combined with the aug-cc-pVTZ basis set yielding an error of 4.25 kcal/mol. The worst average unsigned error among the density functional methods is 15.05 kcal/mol and is obtained using the hybrid-GGA functional B3P86 along with the 3-21+G* basis set. Overall, the largest unsigned error of 26.53 kcal/mol is obtained with the HF/3-21G* method.

Of the three LSDA functionals the best ionization potential unsigned error of 7.46 kcal/mol is obtained using the SPL/cc-pVDZ method. Among the GGA functionals G96P86/cc-pVTZ yields the lowest unsigned error of 4.93 kcal/mol, it should also be noted that the PW91PW91/cc-pVTZ, PBEP86/cc-pVTZ, PBEPW91/aug-cc-pVTZ, and PBEPBE/aug-cc-pVTZ methods all yield errors lower than 5.00 kcal/mol. The B98/aug-cc-pVTZ method yields an average unsigned error of 4.65 kcal/mol, the lowest unsigned error among all hybrid-GGA methods. The functional/basis set combination yielding the best result in the meta-GGA class of functionals is MPWB95/aug-cc-pVTZ with a calculated value of 4.38 kcal/mol. Among the hybrid-meta-GGA functionals the lowest average unsigned error is given by the B1B95/aug-cc-pVTZ method with a value of 4.25 kcal/mol.

As in the case of electron affinities, the Hartree-Fock method does a very poor job in predicting ionization potentials, this can be explained in the same way as above. The cation has fewer electrons than the neutral systems and, thus, exhibits less correlation effects. The Hartree-Fock method's inability to describe electron correlation will lead to a more accurate prediction for the electronic energy of the cation as compared to the neutral species.

As one might expect, the small, 3-21G* and 3-21+G*, basis sets typically perform very poorly in predicting ionization potentials compared to the larger basis sets. Generally the 3-21+G* basis set predicts average errors that are substantially lower than the 3-21G* basis set. The best ionization potential result for the 3-21G* basis set is obtained with the hybrid-GGA B3LYP functional with an average error of 7.33 kcal/mol while the 3-21+G* basis set has an its lowest average unsigned error of 5.26 kcal/mol when used in conjunction with the meta-GGA BB95 functional.

Inspection of the average unsigned errors for individual functionals in Figure 8 and Figure 9 and in Table 3 reveals that the cc-pVTZ, 6-31+G*, 6-31++G*, aug-cc-pVDZ, and aug-cc-pVTZ basis sets all yield fairly similar results that are typically superior to the results obtained with the 3-21G*, 3-21+G*, 6-31G*, and cc-pVDZ basis sets. An exception to this is the LSDA functionals, for which the 6-31G* and cc-pVDZ basis sets yield the lowest average unsigned errors. As the Pople type 6-31+G* and 6-31++G* basis sets are computationally much less expensive to use compared to the larger Dunning correlation consistent basis sets, it is very promising, in terms of biological applications, that such high quality results can be obtained using the smaller basis sets. It should be noted that the MPWB95/(6-31+G*, 6-31++G*) methods (4.53 kcal/mol, 4.50 kcal/mol) outperform all other meta-GGA methods with the exception of the MPWB95/(cc-pVTZ, aug-ccpVTZ) methods (4.49 kcal/mol, 4.38 kcal/mol). Similarly, the B1B95/(6-31+G*, 6-31++G*) methods (4.81 kcal/mol, 4.80 kcal/mol) yield better results than all other hybrid-meta-GGA methods with the exception of B1B95/(aug-cc-pVDZ, cc-pVTZ, aug-cc-pVTZ) methods (4.64 kcal/mol, 4.53 kcal/mol, 4.25 kcal/mol). For the 6-31++G* basis set, the best GGA result of 5.07 kcal/mol is obtained with the PBEPW91 functional. The best hybrid-GGA result for Pople type basis sets is 5.05 kcal/mol and is obtained with the B98/6-31+G* method.

As with the electron affinities, the addition of diffuse functions to hydrogen atoms in the 6-31 ++G* basis set seems to have a negligible effect on the calculation of ionization potentials compared to the 6-31+G* basis set. There is also only a small difference between the results obtained with the cc-pVTZ and aug-cc-pVTZ basis sets. There is, however, a marked difference in the quality of the cc-pVDZ and aug-cc-pVDZ basis set results.

3.6 Heats of Formation

Unsigned errors for the heat of formation (HOF) test set are listed in Figure 10 and Figure 11 along with Table 3. Overall, the combination that gives the lowest unsigned error is PBE1KCIS/ aug-cc-pVTZ at 3.64 kcal/mol. Neglecting errors from the LSDA, MP2, and HF methods, the overall least accurate combination is PW91P86/6-31G* with an average unsigned error of 51.4 kcal/mol. The MPWLYP/3-21G* method yields an unsigned error of 5.66 kcal/mol which is the lowest error for the relatively inexpensive 3-21G* and 3-21+G* basis sets.

For the Pople basis sets, the accuracy of HOF calculations is dependent on the size of the basis set for the hybrid-GGA and meta-hybrid GGA classes of functionals. As shown in Figure 10, the all of the meta-hybrid GGA functionals and all but one of the hybrid-GGA functionals yield much higher errors for the 3-21G* and 3-21+G* basis sets than for the 6-31G*, 6-31+G*, and 6-31++G* basis sets while the other functional classes show no such dependency. The use of diffuse basis sets with GGA and meta-GGA functionals appears to increase the accuracy of the methods as 3-21+G*, 6-31+G*, and 6-31++G* produce typically lower HOF errors than their non-diffuse counterparts. The opposite effect is observed when diffuse bases are paired with hybrid-GGA or hybrid-meta-GGA functionals. The most accurate functional/basis combination within the set of Pople bases is TPSSKCIS/6-31+G*, yielding an average unsigned error of 4.76 kcal/mol.

Generally, the hybrid-meta-GGA class of functionals produces the most accurate HOF calculations. Within this class B1B95/6-31G* yields the most accurate results with a 5.03 kcal/ mol average unsigned error. For all five functionals in this class, the 6-31G* basis is the most accurate of the Pople type bases. The meta-GGA class of functionals yields errors slightly larger than those of the hybrid-meta-GGA class, on the whole. Functionals employing the TPSS exchange perform the best in this class. BB95 also performs well. TPSSTPSS/6-31+G* and TPSSKCIS/6-31+G* are the most accurate combinations within this functional category, producing average errors of 4.76 kcal/mol. The 6-31+G* basis yields the lowest error for each of the functionals in this class. Within the hybrid-GGA class, no functional's performance is particularly good. Within the GGA family, the P86 correlation term should be avoided as these data suggest that it is generally ill-suited for HOF calculations. Four functionals, PBELYP, MPWLYP, MPWPW91, and MPWPBE perform very well. With the exception of MPWP86, all functionals containing the MPW exchange perform well. MPWLYP/3-21G* gives the most accurate results of the entire class with an average unsigned error of 5.66 kcal/mol, which is remarkable for such an inexpensive method. The accuracy of this method surpasses that of many of the more expensive methods included in this study. As seen in Figure 10, the 6-31G* basis generally produces the highest average errors with a few exceptions.

As seen in Figure 11, the Dunning-style correlation-consistent basis sets yield a smaller range of errors than the Pople-style bases. This may be due to the fact that the cc-pVDZ basis, the smallest Dunning-style basis used, is still quite large and is more accurate than the 3-21G* and 3-21+G* bases. As discussed previously, enthalpy calculations were preformed at the same functional/basis combination as the geometry optimization of each molecule, the exception being aug-cc-pVTZ, for which single point enthalpy calculations were performed at the TPSS1KCIS/aug-cc-pVDZ geometries. The lowest average error for all Dunning-style bases is obtained with B3PW91/aug-cc-pVTZ at 3.95 kcal/mol. Within each class of functional there is a mixture of accurate and inaccurate methods.

Within the hybrid-meta-GGA class, MPW1KCIS is the most accurate; with the MPW1KCIS/
cc-pVTZ method producing an average error of 3.97 kcal/mol. Augmentation of the bases with
diffuse functions tends to reduce the accuracy of methods in this functional class. Once again,
the meta-GGA functionals prove to be the second most accurate DFT methods for HOF
calculation. On the whole, the TPSSKCIS and TPSS methods produce the best results among
meta-GGA functionals. However, VSXC/aug-cc-pVDZ is the most accurate combination in
the class with an average unsigned error of 3.98 kcal/mol. The use of DZ versus TZ bases does
not seem significant within this class, as the TZ bases produces the largest errors in three of
the seven functionals. The hybrid-GGA class of functionals reveals the same trends with the
Dunning-type bases as with the Pople bases. PBE1PBE is most accurate functional, and
B3PW91/aug-cc-pVTZ produces the lowest error at 3.95 kcal/mol. Within this class, the
expansion of the basis set from DZ to TZ does not enhance the accuracy of the HOF calculations
as the TZ bases produce nearly equivalent errors for all functionals in the set. The behavior of
the GGA class of functionals with the Dunning type basis sets is again similar to that of the
Pople bases. Methods containing the P86 correlation term are again very poor at predicting
heats of formation, while those containing the MPW exchange term are more accurate. BPW91
also performs well compared to the rest of the functionals in this group. The most accurate
method within this class is HCTH/aug-cc-pVDZ, which produces an average error of 6.83 kcal/
mol. Twelve of the sixteen functionals in the class show a decrease in accuracy with the addition
of diffuse functions. Again, there is little difference in values obtained with DZ bases as
opposed to TZ methods, as most functionals show only a slight increase in accuracy when
using the TZ bases instead of the DZ sets.

Of the LSDA methods, c-SVWN5 performs notably well at predicting heats of formation. c-
SVWN5/3-21+G* yields an average unsigned error of 9.44 kcal/mol, the best value in this
group. In terms of heat of formation, c-SVWN5 is 4 to 13 times more accurate than other LSDA
methods. Other LSDA methods do not accurately predict HOF.

3.7 Hydrogen Bonding Interaction Energies

Figure 12 and Figure 13 give the average hydrogen bonding interaction energy unsigned errors
for gradient corrected density functional methods along with Pople and Dunning type basis
sets respectively. Table 4 gives the average unsigned hydrogen bond interaction errors for HF,
MP2, and LSDA functional methods. Overall the best result is obtained with MP2/aug-cc-
pVDZ with an average error of 0.25 kcal/mol. The best result among density functional
methods is 0.31 kcal/mol as obtained by MPWLYP/aug-cc-pVTZ. The largest overall error of
10.26 kcal/mol is obtained by the c-SVWN5/aug-cc-pVDZ method.

Not surprisingly, the small Pople type basis sets, 3-21G* and 3-21+G*, generally yield poor
results in terms of hydrogen bonding. For most functionals, the errors obtained with these small
bases are greater than 2.00 kcal/mol. Some notable examples of small basis methods that
perform fairly well are HCTH/3-21+G* (0.84 kcal/mol), G96LYP/3-21+G* (0.90 kcal/mol),
and MP2/3-21+G* (0.85 kcal/mol). The best result for these small basis sets combined with one
of the LSDA methods, which are very computationally inexpensive, is 7.99 kcal/mol as
calculated using c-SVWN5/3-21G*.

As one might expect, the 6-31+G* and 6-31++G* basis sets, which contain diffuse functions,
generally outperform 6-31G* in terms of hydrogen bonding, there are seven methods for which
this is not the case, these are HF, BPW91, G96LYP, G96P86, VSXC, BB95, and B1B95.
Somewhat surprisingly there is typically only a small advantage to using the 6-31++G* basis
set, which incorporates diffuse functions for hydrogen atoms, as compared to the 6-31+G*
basis set.

For the large Pople type basis sets, the MP2 method performs very well with average unsigned binding energies of 0.28 kcal/mol and 0.29 kcal/mol with 6-31++G* and 6-31+G* respectively (these values represent the second and third best overall results). Hartree-Fock performs fairly well with these basis sets with a best value of 0.91 kcal/mol when combined with 6-31G*.

The LSDA functionals perform poorly for hydrogen bonding when combined with the large Pople type basis sets. The SVWN5 and SPL functionals both yield errors greater than 6.00 kcal/mol with these bases. The c-SVWN5 functional, which gives results that are substantially better than those of the other two LSDA methods, still only yields a best result of 4.85 kcal/mol (with both the 6-31+G* and 6-31++G* basis sets).

There is a great deal of variation in the hydrogen bonding results obtained with the GGA functionals. The lowest interaction energy error of 0.46 kcal/mol is obtained with the MPWPW91 functional combined with both the 6-31+G* and 6-31++G* basis sets. The highest error of 2.59 kcal/mol is given by PW91P86/6-31G*. Other noteworthy methods in this class are MPWPBE/(6-31+G*,6-31++G*) (0.47 kcal/mol) and BLYP/6-31++G* (0.55 kcal/mol). It is interesting to note that, generally, functionals containing the P86 correlation functional perform poorly while functionals containing the MPW exchange functional perform fairly well when used along with the large Pople type basis sets. The MPWP86 functional performs moderately well with an average error of 1.03 kcal/mol for MPWP86/6-31++G*.

For the large Pople type basis sets, the best result among hybrid-GGA methods is 0.33 kcal/mol as calculated with the B1LYP/6-31++G* method, it should also be noted that this is the best overall result for these basis sets among density functional methods. B1LYP/6-31+G* gives a slightly higher average unsigned interaction energy of 0.34 kcal/mol while B3LYP also performs well with average errors of 0.36 kcal/mol and 0.38 kcal/mol with 6-31+G* and 6-31++G* respectively.

Among the meta-GGA methods the lowest interaction energy error of 0.42 kcal/mol is obtained with the TPSS1KCIS/6-31++G* method. The VSXC functional performs very poorly compared to the other meta-GGA functionals (indeed, it performs poorly compared to most gradient corrected functionals). It is interesting to note that four of the seven functionals in this class obtain errors lower than 0.50 kcal/mol when combined with the 6-31+G* and 6-31++G* basis sets, these functionals are MPWB95, TPSS, MPWKCIS, and TPSSKCIS.

Each of the five hybrid-meta-GGA functionals performs quite well for hydrogen bond interaction energies when paired with the 6-31+G* and 6-31++G* basis sets, with no method obtaining average errors larger than 1.00 kcal/mol. The best result in this class is 0.38 kcal/mol and is given by the MPW1KCIS/6-31++G* method. Other noteworthy methods are BB1K/6-31+G* (0.40 kcal/mol), BB1K/6-31++G* (0.41 kcal/mol), MPW1KCIS/6-31++G* (0.42 kcal/mol), and TPSS1KCIS/6-31+G* (0.42 kcal/mol).

As in the case of the Pople type basis sets, the Dunning type basis sets that contain diffuse functions, aug-cc-pVDZ and aug-cc-pVTZ, yield better hydrogen bond interaction energies than the ones that do not, cc-pVDZ and cc-pVTZ, for a majority of the functionals considered in this work. Generally speaking the cc-pVTZ functional outperforms the, smaller, cc-pVDZ basis set for hydrogen bonding, it should be noted that this is not the case for Hartree-Fock or any of the LSDA functionals. The aug-cc-pVTZ typically outperforms the aug-cc-pVDZ basis set for LSDA, GGA, and hybrid-GGA functionals while the smaller basis, aug-cc-pVDZ, yields better results when combined with the meta-GGA and hybrid-meta-GGA functionals.

The Hartree-Fock method yields fairly large errors with the Dunning type basis sets, with the lowest unsigned error being 1.65 kcal/mol for HF/cc-pVDZ and the highest being 1.77 kcal/mol for HF/cc-pVTZ. These values are significantly higher than those obtained with the large

Pople type basis sets. The MP2 method performs very well with most Dunning type basis sets, MP2/aug-cc-pVDZ produces an average unsigned error of 0.25 kcal/mol, which is the best value obtained for hydrogen bond interaction energies obtained in this work.

Once again the LSDA functionals perform very poorly compared to the other DFT methods. Among these methods, the SPL and SVWN5 functionals generally yield results that are almost identical for all Dunning type basis sets. The c-SVWN5 method yields unsigned errors that are significantly higher than those of SPL and SVWN5. The best LSDA result of 5.48 kcal is obtained with SPL/cc-pVDZ. The worst LSDA result is given by c-SVWN5/aug-cc-pVDZ with a value of 10.26 kcal/mol.

Among the GGA methods, the Dunning type basis sets outperform the large Pople type bases for nine of the sixteen functionals. The MPWLYP functional performs significantly better than all other functionals in this class with the best value of 0.31 kcal/mol given by MPWLYP/aug-cc-pVTZ. The highest unsigned error of 2.78 kcal/mol is obtained with the G96LYP/cc-pVDZ method. Both functionals containing the G96 correlation functional, G96LYP and G96P86, give very poor results with errors that are greater than 2.00 kcal/mol for all Dunning type basis sets.

For the hybrid-GGA methods, four of the six functionals, B1LYP, B3LYP, PBE1PBE, and B3P86, obtain errors that are between 0.50 kcal/mol and 0.80 kcal/mol, the remaining functional, B3PW91, does not perform as well, producing errors that are above 1.00 kcal/mol for all basis sets. For all Dunning type basis sets, the B98 functional produces the best hydrogen bonding results. The best result within this class is given by the B98/aug-cc-pVDZ method, with a value of 0.40 kcal/mol.

Among the meta-GGA methods, PBEKCIS stands out as being notably better than all other functionals. Values of 0.32 kcal/mol and 0.34 kcal/mol are obtained when PBEKCIS is combined with the aug-cc-pVDZ and aug-cc-pVTZ basis sets respectively, these are the lowest unsigned errors within this class. The VSXC and BB95 functionals both perform poorly.

Within the hybrid-meta-GGA class of functionals, PBE1KCIS yields the lowest errors for hydrogen bonding interaction energies for all Dunning type basis sets. The best result in this class is obtained with PBE1KCIS/aug-cc-pVDZ with a value of 0.36 kcal/mol. The next best functional in this class is TPSS1KCIS, whose lowest error is 0.55 kcal/mol at the TPSS1KCIS/aug-cc-pVDZ level.

3.8 Conformational Energies

The average unsigned conformational energy errors are given in Figure 14 and Figure 15 and in Table 4. There are great differences in the conformational energies of the systems considered here, for example the experimental difference in energy between the orthogonal and planar conformers of ethylene is 65.0 kcal/mol whereas the experimental value for the conformational energy for the anti and eclipsed forms of methanol is 1.1 kcal/mol. For this reason, the conformational energies are reported in percent error, that is

$$\text{error}_\% = \frac{\Delta E_{\text{exp}} - \Delta E_{\text{theory}}}{\Delta E_{\text{exp}}} \times 100$$

Overall, the best result of 6.8% is obtained with the MP2/aug-cc-pVDZ method. The best result among density functional methods is 7.9% as calculated using MPWB95/cc-pVTZ. The worst conformational energy error is that of VSXC/3-21G* with a value of 81.9%.

As seen in Figure 14 and Table 4, the small Pople type basis sets, 3-21G* and 3-21+G*, give conformational energy errors that are typically much greater than those of the larger Pople type

basis sets, 6-31G*, 6-31+G*, and 6-31++G*. Generally, 3-21+G* outperforms 3-21G*, there are several exceptions to this rule in the hybrid-GGA and hybrid-meta-GGA classes of functionals, also 3-21G* yields slightly lower errors than 3-21+G* for the GGA functional HCTH. For these small basis sets, the LSDA method produces conformational energies that are significantly worse than those of the gradient corrected density functional methods. The lowest unsigned error for small Pople type basis sets is obtained with the MP2/3-21+G* method with a value of 21.7%, for DFT methods the best value of 23.3% is obtained with the PBELYP/3-21+G* method.

For the Pople type basis sets the best conformational energy results can be found within the meta-GGA and hybrid-meta-GGA functional classes. The best overall result of 12.2% is obtained with the, hybrid-meta-GGA, B1B95/6-31++G* method. It should be noted that although the BB1K and B1B95 methods perform very well, the remaining three functionals in the hybrid-meta-GGA class, MPW1KCIS, PBE1KCIS, and TPSS1KCIS, yield errors that are about two to four percent higher. Within the meta-GGA group of functionals, BB95, MPWB95, and TPSS all yield very low conformational energy errors. The lowest unsigned error in this class is produced by the MPWB95/6-31++G* method with a value of 12.4%. Among the hybrid-GGA functionals, B98 obtains errors that are about one percent lower than those of the next best functional, B3P86. The lowest error in this class is obtained at the B98/6-31++G* level with an average unsigned error of 14.2%. Two GGA functionals, PBEP86 and PW91P86, produce the best results within their class, both yield an error value of 14.0% when paired with the 6-31++G* basis set. Among the LSDA functionals, SPL and SVNWV both yield the same error values of 15.6% and 15.5% when paired with the 6-31+G* and 6-31++G* bases respectively. Hartree-Fock generates errors that are significantly higher than those obtained by most DFT methods, the best error value of 22.1% is obtained with 6-31+G*. The MP2 method obtains errors of 15.5% when paired with 6-31++G* and 16.8% with the 6-31+G* basis set.

The basis sets that include diffuse functions, 6-31+G* and 6-31++G*, generally give unsigned errors that are substantially lower than those obtained using the 6-31G* basis function. It is also interesting to note that 6-31++G* outperforms 6-31+G* for most of the functionals considered here.

Figure 15 and Table 4 give the conformational energy unsigned errors for the Dunning type basis sets. Here it can be seen that there is no class of functional that stands out as being substantially more accurate than another. Some of the lowest unsigned errors are obtained with BB1K and B1B95 (hybrid-meta-GGA), BB95 and MPWB95 (meta-GGA), and with PBEP86 and PW91P86 (GGA). The B98 functional produces the best hybrid-GGA results, which are not quite as good as the best results obtained by other DFT methods. It is also interesting to note that each of the LSDA methods studied here yields results that are competitive with many of those obtained with the, more sophisticated, gradient corrected techniques. Among all density functional methods considered in this work, the lowest unsigned error obtained for this property is 7.9% as calculated using the MPWB95/cc-pVTZ method. Once again, the VSXC functional (meta-GGA) performs very poorly for describing conformational energies. The MP2 method also yields very good results for all Dunning type basis sets except for cc-pVDZ. The best overall conformational energy result obtained in this study is 6.8% and is given by the MP2/aug-cc-pVDZ method. Hartree-Fock produces errors that are significantly higher than those of most DFT techniques.

Among the Dunning type basis sets, aug-cc-pVDZ and cc-pVTZ tend to yield the lowest errors. The aug-cc-pVDZ basis set gives the best results for all of the hybrid-GGA functionals, all of the LSDA functionals, and for all of the hybrid-meta-GGA functionals except MPW1KCIS. The cc-pVTZ basis set yields the lowest unsigned errors for all of the GGA functionals and for all of the meta-GGA functionals except VSXC and MPWKCIS. The cc-pVDZ basis set

produces the largest errors among Dunning type basis sets for each of the computational techniques employed in this study with the exception of VSXC.

3.9 Barrier Heights

a. Barrier heights for reactions of small systems with radical transition states (SRBH)—Figure 16 and Figure 17 give the average unsigned barrier height errors of the SRBH systems for gradient corrected functionals along with the Pople and Dunning type basis sets respectively. Table 4 gives the SRBH barrier height errors for the HF, MP2, and LSDA functional methods along with all basis sets considered in this work. Overall the best result is obtained with the BB1K/aug-cc-pVTZ method with an average unsigned error of 1.05 kcal/ mol. The highest error, 21.95 kcal/mol, is produced with the SVWN5/3-21G* functional/basis combination. Again we would like to point out that these barrier heights are based on single point calculations at geometries determined at the QCISD/MG3 level of theory.

Inspection of these data reveals that the DFT methods that include exact exchange, that is, the hybrid-GGA and hybrid-meta-GGA methods, generally yield the lowest barrier height errors. The LSDA methods, which are based solely on the electron density, produce the largest unsigned errors.

The LSDA, GGA, and meta-GGA perform poorly for SRBH barrier heights. Each of the LSDA methods produces errors larger than twelve kcal/mol for all basis sets. Of the GGA functionals, only HCTH yields errors smaller than six kcal/mol. The best result in this class is obtained with the HCTH/6-31++G* method with an average unsigned error of 4.86 kcal/mol. Among the meta-GGA methods, only the VSXC functional obtains errors smaller than six kcal/mol. The smallest error in this class is 4.24 kcal/mol and is given by the VSXC/6-31++G* method.

Among the hybrid-GGA functionals, B1LYP yields the smallest errors for all basis sets, this functional produces its lowest error of 3.11 kcal/mol when paired with the aug-cc-pVTZ basis set. It should be noted that B1LYP/6-31++G* gives a slightly higher error of 3.23 kcal/mol. In the hybrid-meta-GGA class, the BB1K functional stands out as clearly being the best performer, indeed, for each basis set, this functional produces the best results among all methods considered in this work. The lowest error in this class is obtained with the BB1K/aug-cc-pVTZ method with a value of 1.05 kcal/mol. The next best functional for the calculation of these SRBH barrier heights is B1B95, which produces the second best results among all methods studied here. The lowest error given by this functional is 2.64 kcal/mol as calculated using the 6-31G* basis set.

The Hartree-Fock method performs very poorly in describing radical transition state barrier heights, the lowest unsigned error attained with this technique is 10.78 kcal/mol, with the 3-21 +G* basis set. MP2 yields fairly good results when paired with the Dunning type basis sets but, when paired with the Pople type basis sets, produces much larger errors. The lowest unsigned error attained with this method is 2.98 kcal/mol at the MP2/aug-cc-pVDZ level.

b. Barrier heights for reactions of large systems with singlet transition states (LSBH)—Figure 18 and Figure 19 and Table 4 show the reaction barrier heights for the six reactions listed in the LSBH test set. Transition state barrier heights in this study are calculated as the difference between temperature-corrected total enthalpy of the transition state and that of the reactants. All structures have been fully optimized at each functional/basis set combination. The values listed in the following tables are average values of the error in transition state barrier height over all six reactions considered. These reactions include: 1) Diels-Alder reaction of butadiene and ethene forming cyclohexene 2) Cope rearrangement of 1,5 hexadiene 3) Claisen rearrangement of allyl vinyl ether to pentenal 4) the electro-cyclic

rearrangement of cyclobutene to butadiene 5) 1,5-sigmatropic shift of 2,4 pentanedione and 6) the 1,5-sigmatropic shift of 1,3-pentadiene.

Overall, the functional that provides the lowest average error over all six reactions for both Pople and Dunning basis sets is B1LYP. The average error for this functional is 2.63 kcal/mol for the 6-31++G* basis and 2.58 kcal/mol for the aug-cc-pVTZ basis. Generally, a marked improvement in accuracy is observed between basis sets for each functional. The 3-21G* and 3-21+G* are less accurate than the larger Pople-type bases by 3-4 kcal/mol, while the triple-zeta Dunning-style basis sets are more accurate than their double-zeta counterparts by nearly . 5 kcal/mol. The hybrid-GGA and hybrid-meta GGA functional classes perform markedly better for predicting barrier heights than the LSDA, GGA, and meta-GGA classes. This result indicates a trend that is the opposite of that observed for frequency calculations, for which functionals that include the Hartree-Fock exact exchange perform worse than those without a DFT "exact exchange" term. Since frequency calculations must be performed for transition state optimizations this result is somewhat surprising. Moreover, on it's own, the HF method is more accurate than most DFT methods at predicting barrier heights when the 3-21G* and 3-21+G* basis sets are used. MP2 also performs well with the lower basis sets. In fact, for HF, basis sets larger than 3-21G* produce errors nearly twice as large as those given by the smallest bases.

Among the LSDA functionals, c- SVWN5 functional gives the greatest accuracy, while SPL is slightly less accurate. The average barrier height error for c-SVWN5/cc-pVDZ is 11.22 kcal/ mol. Typically average errors within the LSDA class are near 12 kcal/mol except for the lower Pople style basis sets, which returned errors from 18–20 kcal/mol for the SPL and SVWN5 functionals.

Within the GGA class, most functionals yield similar results, while the HCTH functional clearly returning the most accurate results. As mentioned, the accuracy of the barrier height calculations is highly basis set dependent for the Pople-type basis sets. HCTH/6-31+G* and HCTH/6-31++G* both yield an average error of 4.15 kcal/mol over all six reactions, while HCTH/cc-pVTZ produced an average error of 4.05 kcal/mol. For the class as a whole, errors for the 3-21G* and 3-21+G* average 9-13 kcal/mol while errors for the larger Pople bases average 6-8 kcal/mol. The Dunning basis sets provide accuracy equivalent to the high level Pople sets. Similar results are obtained by the meta-GGA class, in which VSXC is by far the most accurate. Once again the lower Pople basis sets yield average errors of 8-11 kcal/mol, while the larger Pople sets and the correlation-consistent sets give average errors of 7-8 kcal/ mol. The VSXC functional consistently yields lower errors than the other functionals in this class.

Hybrid-GGA methods perform better than either the GGA or meta-GGA methods, with B1LYP proving to be the most accurate functional tested. Again a large dependence on the basis is observed with the Pople-type basis sets as the larger basis sets are much more accurate than 3-21G* and 3-21+G*. TZ Dunning-type sets are slightly more accurate than the DZ sets. B1LYP/6-31++G* and B1LYP/aug-cc-pVTZ are the most accurate functional/basis combinations in the entire test set, producing average errors of 2.63 and 2.58 kcal/mol, respectively. B3LYP also provides very accurate calculations for the barrier height test set. On the whole, the hybrid-GGA and hybrid-meta-GGA classes provide similar accuracy. Of the hybrid-meta-GGA class, BB1K yields the lowest average errors with the Pople-type bases, while B1B95 performs better when the Dunning-style sets are employed.

4. Conclusions

In terms of geometric parameters hybrid-GGA and hybrid-meta-GGA generally yield the best results for both bond lengths and bond angles. The LSDA functionals generally do not perform as well as the more sophisticated functionals. The choice of basis set has a large impact on the quality of calculated geometric parameters. In terms of bond lengths, the large Pople type basis sets, 6-31G*, 6-31+G*, and 6-31++G*, generally perform similarly to or better than the much larger (and more expensive) cc-pVDZ and aug-cc-pVDZ basis sets for all gradient corrected functionals. For bond angles, the Dunning type basis sets generally yield the best results. The largest of these bases, augcc-pVQZ, generally obtains the lowest bond angle errors for all DFT functional classes. The large Pople type basis sets that incorporate diffuse functions typically yield bond angles that are only slightly less accurate than those obtained with the aug-cc-pVDZ and cc-pVTZ basis sets. For most functionals, 6-31++G* produces bond angle errors that are only 0.01° to 0.05° higher than those of aug-cc-pVDZ.

The methods that include DFT "exact exchange" perform very poorly for calculating the vibrational frequencies of molecules. For large Pople and Dunning type basis sets, these methods generally yield unsigned frequency errors that are 1.5 to 2 times larger than those obtained with method that do not include exact exchange. For all basis sets, with the exception of 3-21G*, the GGA functionals produce the lowest average frequency errors. For LSDA and GGA functionals, the augmented Pople type basis sets, 6-31+G* and 6-31++G*, typically produce errors that are slightly lower than those of aug-cc-pVDZ and slightly higher than those of aug-cc-pVTZ. For all functionals, the Pople-type basis sets yield errors that are comparable to the errors computed using all Dunning-type basis sets.

For electron affinities there is no strong tendency for one functional class to significantly outperform another, with the exception of LSDA, which performs very poorly compared to all other functional groups. It is interesting to note that all functionals containing the P86 correlation functional (GGA and hybrid-GGA) perform very poorly. Functionals incorporating "exact exchange" tend to yield the smallest errors when combined with larger Dunning-type basis sets while the other functional groups, LSDA, GGA, and meta-GGA, all obtain the most accurate results when used in conjunction with the 6-31+G* and 6-31++G* basis sets.

For ionization potentials the best results are obtained with the hybrid-meta-GGA functionals. It is very promising, in terms of large-scale calculations, that the ionization potential results obtained with the 6-31+G* and 6-31++G* basis sets are comparable to those obtained using the much larger Dunning-type basis sets for most functionals. As one might expect, the inclusion of diffuse functions in the basis set greatly improves the results for this property.

For heats of formation, the meta-GGA and hybrid-meta-GGA classes of DFT functionals appear to be the most accurate. It is important to note that in all classes except LSDA, one can find some functional/basis combination that performs well. Overall, the Dunning-style bases are more accurate than the Pople-type sets, with the cc-PVTZ and aug-cc-pVTZ bases yielding the lowest average unsigned errors for our 156-molecule heat of formation test set. However, it should be noted that one can achieve a very high level of accuracy with the MPWLYP/3-21G* method. This combination produces an average error of only 5.6 kcal/mol, which is only 2 kcal/mol less accurate than the best result obtained within the entire study. Within the GGA class of functionals, a wide range of accuracies is obtained.

Generally the hybrid-GGA, meta-GGA, and hybrid-meta-GGA functionals yield the best results for hydrogen bond interaction energies. There is a large amount of variation among the GGA functionals, with some giving very good results and others performing very poorly. The MP2 method produces some of the lowest hydrogen bonding interaction energy errors. For both the large Pople type basis sets and the Dunning type bases the addition of diffuse

functionals typically produces lower unsigned errors. The inlusion of diffuse functions on hydrogen atoms in the 6-31++G* basis does not generally increase the performance in terms of hydrogen bonding interaction energies when compared to the 6-31+G* basis. For the large Pople and Dunning type bases that include diffuse functions, there is no clear tendency for one particular basis set to consistently produce the lowest errors within the GGA class of functionals, for all of the other functional classes the 6-31+G* and 6-31++G* bases generally give the best results.

In terms of conformational energies, the meta-GGA and hybrid-meta-GGA functionals produce the lowest average errors. Not surprisingly, the large Pople type basis sets, 6-31G*, 6-31+G*, and 6-31++G*, yield results that are typically about ten percent better than those obtained using the smaller Pople type bases, 3-21G* and 3-21+G*. For the large Pople type basis sets there is a slight improvement in the calculated conformational energies when diffuse functionals are employed. Overall the basis sets that produce the lowest errors are the Dunning type bases, aug-cc-pVDZ and cc-pVTZ.

One of the most salient aspects of the data concerning the barrier heights of small molecules with radical transition states (SRBH) is that functionals containing exact exchange terms generally produce the lowest average barrier height errors. The LSDA methods, which depend only on the electron density, produce errors that are significantly higher than those of all other methods considered here. In terms of basis sets, the inclusion of diffuse functions typically increases the accuracy with which the barrier heights of these reactions can be calculated. The lowest barrier height errors are generally produced with the 6-31+G*, 6-31++G*, and aug-cc-pVTZ bases.

As in the case of the SRBH reactions, the barrier heights of larger systems with singlet transition states (LSBH) are generally better described by functionals that contain exact exchange. The addition of diffuse functions to the 3-21G*, 6-31G*, and cc-pVTZ basis sets generally results in a lower unsigned average error, in the case of the cc-pVDZ basis set however, the addition of diffuse functions typically increases the errors slightly. For the LSBH reactions, the 6-31 +G*, 6-31++G*, and aug-cc-pVTZ basis sets generally produce the lowest errors for most methods studied in this work.

Here, we will attempt to summarize the results obtained in the entire study and draw some conclusions concerning the functionals that seem to offer the best compromise in terms of describing all of the physical properties investigated in this work. As we have generated a tremendous amount of data in this study, we will limit our discussion by considering only the results obtained by two popular basis sets, 6-31+G* and aug-cc-pVDZ.

One of the most interesting observations that can be made from the data presented here is that, for many physical properties, the large Pople-type basis sets (6-31G*, 6-31+G*, and 6-31+ +G*) produce results that are comparable to, or superior to, those given by the much larger and computationally expensive Dunning-type basis sets. For example, for the B1B95 functional, the 6-31+G* basis set outperforms the aug-cc-pVDZ basis set for bond distances, heats of formation, hydrogen bond interaction energies, and reactions barrier heights (both SRBH and LSBH); the average unsigned bond angle error obtained with the smaller basis set is only 0.034° higher than that of the larger basis and the average unsigned ionization potential error for 6-31+G* is only 0.28 kcal/mol larger than that of aug-cc-pVDZ. The average unsigned electron affinity, vibrational frequency and conformational energy errors are larger for 6-31 +G* than for aug-cc-pVDZ.

Table 5 indicates the rankings of the top five functional/basis set combinations overall and the top three functional/basis set combinations among Pople-type basis sets for each property considered in this work. In table 5 it can be seen that for each physical property considered

here, with the exception of conformational energies, the best results obtained with Pople-type basis sets are comparable to the best results produced by the larger Dunning-type bases.

One of the main goals of this survey is to get a rough estimate of a functional's performance in terms of its ability to describe all of the properties considered in this study. In order to accomplish this goal we compare the average functional ranks and standard deviations for each of the functionals studied in this work. The average functional rank is given as the mean of a functional's rank for all of the properties considered here and the standard deviation was also calculated.

Table 6 lists the average functional ranks and standard deviations of the fifteen functionals with the lowest average ranks for the 6-31+G* and aug-cc-pVDZ basis sets. For both basis sets there are five hybrid-meta-GGA and three meta-GGA functionals represented in the "top fifteen". The top fifteen of the 6-31+G* basis also included four hybrid-GGA and three GGA functionals, while the top performers from the aug-cc-pVDZ set included five hybrid-GGA and two GGA functionals. In the aug-cc-pVDZ group, each of the "top five" functionals in terms of average functional rank contains "exact exchange" terms. Whereas the only three of the "top five" of the 6-31+G* set contain an "exact-exchange" term. Also, for both basis sets, the only GGA functional to rank in the top ten is MPWPW91/aug-cc-PVDZ.

Table 7 lists the fifteen best functionals for the 6-31+G* basis set along with their unsigned errors for each of the properties considered in this work, for purposes of comparison, the lowest and highest unsigned errors for each property are given, as well as the mean unsigned error averaged over all of the functionals in this study. For the 6-31+G* basis set, the B1B95 functional obtains the lowest average functional rank with a value of 10.7. However, the standard deviation of this functional is fairly high with a value of 11.9, since the method performs very well for some properties and relatively poorly for others, as can be seen in Table 7. Other functionals that perform notably well are B98, TPSSTPSS, TPSS1KCIS, and PBE1PBE; each of these functionals gives reasonably good results for all of the physical properties here (with the possible exception of vibrational frequencies).

Table 8 lists the fifteen best functionals for the aug-cc-pVDZ basis set along with their unsigned errors for each of the properties considered in this work in the same manner as was done for the 6-31+G* basis. For this basis set there are a number of functionals that perform very well in terms of giving a good description of each of the physical properties in this work. The B98 functional has the lowest average functional ranking with a value of 10.1 (standard deviation = 8.8). When paired with aug-cc-pVDZ, B98 ranks in the top eleven functionals for all properties except HOF and vibrational frequency. B98's predicted heat of formation is in error by an average of 18.38 kcal/mol. TPSS1KCIS, which ranks as third best with the DZ basis, predicts HOF very well, but is less accurate for electron affinity, conformational energy, and vibrational frequency. Other functionals of note are B1B95, PBE1PBE, and B3LYP.

Supplementary Material

Refer to Web version on PubMed Central for supplementary material.

Acknowledgements

References

1. Adesokan AA, Fredj E, Brown EC, Gerber RB. Mol. Phys 2005;103:1505–1520.

2. Basheerl MM, Perles CE, Volpe PLO, Airoldi C. J. Sol. Chem 2006;35:625–637.

3. Bassan A, Borowski T, Pelmenschikov V, Schofield C, Siegbahn P. Abstracts of Papers of the American Chemical Society 2005;229:U800–U800.

4. Blomberg M, Siegbahn P. Biochimica Et Biophysica Acta-Bioenergetics 2004;1658:145–145.

5. Chen BG, Zhang MY, Zhao YY, Zhang J, Sun CC. Chemical Journal of Chinese Universities-Chinese 2006;27:1307–1310.

6. Dannenberg JJ. Peptide Solvation and H-Bonds 2006;72:227.−+

7. Dannenberg JJ, Asensio A, Kobko N. Abstracts of Papers of the American Chemical Society 2003;226:U330–U330.

8. Dobes P, Otyepka M, Strnad M, Hobza P. Chemistry-a European Journal 2006;12:4297–4304.

9. Dolker N, Maseras F, Lledos A. J. Phys. Chem.B 2003;107:306–315.

10. Dorcier A, Dyson PJ, Gossens C, Rothlisberger U, Scopelliti R, Tavernelli I. Organometallics 2005;24:2114–2123.

11. Ferretti V, Pretto L, Tabrizi MA, Gilli P. Acta Crystallographica Section B-Structural Science 2006;62:634–641.

12. Isaev A, Scheiner S. J. Phys. Chem.B 2001;105:6420–6426.

13. Otyepka M, Sklenovsky P, Horinek D, Kubar T, Hobza P. J. Phys. Chem. B 2006;110:4423–4429. [PubMed: 16509744]

14. Piana S, Bucher D, Carloni P, Rothlisberger U. J. Phys. Chem. B 2004;108:11139–11149.

15. Reha D, Valdes H, Vondrasek J, Hobza P, Abu-Riziq A, Crews B, de Vries MS. Chemistry-a European Journal 2005;11:6803–6817.

16. Rovira C, Parrinello M. Chemistry-a European Journal 1999;5:250–262.

17. Sponer J, Jurecka P, Hobza P. J. Am. Chem. Soc 2004;126:10142–10151. [PubMed: 15303890]

18. Sulpizi M, Folkers G, Rothlisberger U, Carloni P, Scapozza L. Quantitative Structure-Activity Relationships 2002;21:173–181.

19. Szyczewski A, Pietrzak J, Mobius K. Acta Physica Polonica A 2005;108:119–126.

20. Viswanathan R, Asensio A, Dannenberg JJ. J. Phys. Chem. A 2004;108:9205–9212.

21. Wieczorek R, Dannenberg JJ. J. Am. Chem. Soc 2004;126:14198–14205. [PubMed: 15506786]

22. Wieczorek R, Dannenberg JJ. J. Am. Chem. Soc 2005;127:17216–17223. [PubMed: 16332068]

23. Wieczorek R, Dannenberg JJ. J. Am. Chem. Soc 2005;127:14534–14535. [PubMed: 16231881]

24. Xu LZ, Huang YW, Yu GP, Si GD, Zhu Q. Struct. Chem 2006;17:235–239.

25. Zhou WQ, Yang W, Qiu LH. Theochem 2005;130:133–141.

26. Van Alsenoy C, Yu CH, Peeters A, Martin JML, Schafer L. J. Phys. Chem. A 1998;102:2246–2251.

27. Bour P, Kubelka J, Keiderling TA. Biopolymers 2002;65:45–59. [PubMed: 12209472]

28. Jalkanen KJ, Elstner M, Suhai S. Theochem 2004;675:61–77.

29. Oldfield E. Phil. Trans. Royal Soc. B 2005;360:1347–1361.

30. Kohn W, Sham LJ. Phys. Rev 1965;140:A1133–A1138.

31. Hohenberg P, Kohn W. Phys. Rev 1964;136:B864–B871.

32. Perdew, JP.; Schmidt, K. AIP Conf. Proc; 2001. p. 1-20.

33. Mattsson A. Science 2002;298:759–760. [PubMed: 12399569]

34. Seidl M, Perdew JP, Kurth S. Phys. Rev. Lett 2000;84:5070–5073. [PubMed: 10990869]

35. Seidl M, Perdew JP, Kurth S. Phys. Rev. A 2000;62:012502/012501–012502/012515.

36. Binkley JS, Pople JA, Hehre WJ. J. Am. Chem. Soc 1980;102:939–947.

37. Gordon MS, Binkley JS, Pople JA, Pietro WJ, Hehre WJ. J. Am. Chem. Soc 1982;104:2797–2803.

38. Pietro WJ, Francl MM, Hehre WJ, Defrees DJ, Pople JA, Binkley JS. J. Am. Chem. Soc 1982;104:5039–5048.

39. Hehre WJ, Ditchfie R, Pople JA. J. Chem. Phys 1972;56:2257–2261.

40. Dunning TH. J. Chem. Phys 1989;90:1007–1023.

41. Raymond KS, Wheeler RA. J. Comp. Chem 1999;20:207–216.

42. Zhao Y, Schultz NE, Truhlar DG. J Chem Phys 2005;123:161103. [PubMed: 16268672]

43. Zhao Y, Schultz NE, Truhlar DG. J Chem Theory Comput 2006;2:364–382.

44. Scuseria, GE.; Staroverov, VN. Progress in the development of exchange-correlation functionals. In: Dykstra, CE.; G, F.; Kim, KS.; Scuseria, GE., editors. Theory and Applications of Computational Chemistry: The First 40 Years (A Volume of Technical and Historical Perspectives). Amsterdam: Elsevier; 2005. p. 669-724.

45. Wang NX, Wilson AK. J. Chem. Phys 2004;121:7632–7646. [PubMed: 15485223]

46. Wang NX, Wilson AK. Mol. Phys 2005;103:345–358.

47. Bauschlicher CW. Chem. Phys. Lett 1995;246:40–44.

48. Neugebauer A, Häfelinger G. Journal of Molecular Structure-Theochem 2002;578:229.

49. Neugebauer A, Häfelinger G. Theochem 2002;585:35–47.

50. Scheiner AC, Baker J, Andzelm JW. J. Comp. Chem 1997;18:775–795.

51. Johnson BG, Gill PMW, Pople JA. J. Chem. Phys 1992;97:7846–7848.

52. Johnson BG, Gill PMW, Pople JA. J. Chem. Phys 1993;98:5612–5626.

53. Riley KE, Brothers EN, Ayers KB, Merz KM. JCTC 2005;1:546–553.

54. Mole SJ, Zhou X, Liu R. J. Phys. Chem 1996;100:14665–14671.

55. Curtiss LA, Raghavachari K, Redfern PC, Pople JA. J. Chem. Phys 1997;106:1063–1079.

56. Curtiss LA, Redfern PC, Raghavachari K, Pople JA. J. Chem. Phys 1998;109:42–55.

57. Curtiss LA, Raghavachari K, Redfern PC, Pople JA. J. Chem. Phys 2000;112:7374–7383.

58. Curtiss LA, Redfern PC, Raghavachari K. J. Chem. Phys 2005;123:124107/124101–124107/124112. [PubMed: 16392475]

59. Curtiss LA, Redfern PC, Rossolov V, Kedziora Z, Pople JA. J. Chem. Phys 2001;114:9287–9295.

60. Lynch BJ, Truhlar DG. J. Phys. Chem. A 2003;107:8996–8999.

61. Brothers EN, Merz KM. J. Phys. Chem. A 2004;108:2904–2911.

62. Rabuck AD, Scuseria GE. Chem. Phys. Lett 1999;309:450–456.

63. Ernzerhof M, Scuseria GE. J. Chem. Phys 1999;110:5029–5036.

64. Hobza P, Sponer J, Reschel T. J. Comp. Chem 1995;16:1315–1325.

65. Paizs B, Suhai S. J. Comp. Chem 1998;19:575–584.

66. Tuma C, Bosese AD, Handy NC. Phys. Chem. Chem. Phys 1999;1:3939–3947.

67. Rappe AK, Bernstein ER. J. Phys. Chem.A 2000;104:6117–6128.

68. Rabuck AD, Scuseria GE. Ther. Chem. Acc 2000;104:439–444.

69. Ireta J, Neugebauer J, Scheffler M. J. Phys. Chem.A 2004;108:5692–5698.

70. Xu X, Goddard WA. J. Chem. Phys.A 2004;108:2305–2313.

71. Helkier A, Klopper W, Helgaker T, Jorgensen P, Taylor PR. J. Chem. Phys 1999;111:9157.

72. Tsuzuki S, Lüthi, HP. J. Chem. Phys 2001;114:3949–3957.

73. Zhao Y, Truhlar DG. JCTC 2005;1:415.

74. Lynch BJ, Zhao Y, Truhlar DG. J. Phys. Chem. A 2003;107:1384–1388.

75. Stamant A, Cornell WD, Kollman PA, Holgren TA. J. Comput. Chem 1995;16:1483.

76. Scheiner P, Fokin AA, Pascal RA Jr, de Meijere A. Organ. Lett 2006;8:3635–3638.

77. Lynch BJ, Truhlar DG. J. Phys. Chem. A 2002;106:842–846.

78. Zhao Y, González-Garcia N, Truhlar DG. J. Phys. Chem. A 2005;109:2012–2018. [PubMed: 16833536]

79. Dickson RM, Becke AD. J. Chem. Phys 2005;123Art. No. 111101/111101–111101/111103

80. Dybala-Defratyka A, Paneth P, Pu JZ, Truhlar DG. J. Phys. Chem. A 2004;108:2475–2486.

81. Lynch BJ, Fast PL, Harris M, Truhlar DG. Journal of Physical Chemistry A 2000;104:4811–4815.

82. Frisch, MJ.; Trucks, GW.; Schlegel, HB.; Scuseria, GE.; Robb, MA.; Chesseman, JR.; Zakrzewski, VG.; Montgomery, JA., Jr; Stratmann, RE.; Burant, J.; Burant, JC.; Dapprich, S.; Millam, JM.; Daniels, AD.; Kudin, KN.; Strain, MC.; Farkas, O.; Tomasi, J.; Barone, V.; Cossi, M.; Cammi, R.;

Mennucci, B.; Pomelli, C.; Adamo, C.; Clifford, S.; Ochterski, J.; Petersson, GA.; Ayala, PY.; Cui, Q.; Morokuma, K.; Malick, DK.; Rabuck, AD.; Raghavachari, K.; Forseman, JB.; Cioslowski, J.; Ortiz, JV.; Baboul, AG.; Stefanov, BB.; Liu, G.; Liashenko, A.; Piskorz, P.; Komaromi, I.; Gomperts, R.; Martin, RL.; Fox, DJ.; Keith, T.; AlLoham, MA.; Peng, CY.; Nanayakkara, A.; Gonzalez, C.; Challacombe, M.; Gill, PMW.; Johnson, BG.; Chen, W.; Wong, MW.; Andres, JL.; Head-Gordon, M.; Replogle, ES.; Pople, JA. Gaussian 03. C.01 ed. Pittsburgh, PA: Gaussian Inc; 2003.

83. Ochterski, JW. Sep 12. Themochemistry in Gaussian: www.gaussian.com

84. NIST. NIST Chemistry Webbook. 2006 September 12;http://webbook.nist.gov/chemistry/

85. Boys SF, Bernardi F. Mol. Phys 1970;19:553–566.

86. Repasky MP, Chandrasekhar J, Jorgensen WL. J. Comp. Chem 2002;23:1601–1622. [PubMed: 12395428]

87. Halgren, Ta. Journal of Computational Chemistry 1999;20:730–748.

88. Freile ML, Risso S, Curaqueo A, Zamora MA, Enriz RD. Journal of Molecular Structure-Theochem 2005;731:107–114.

89. Zhong HZ, Stewart EL, Kontoyianni M, Bowen JP. Journal of Chemical Theory and Computation 2005;1:230–238.

90. Roothan . Rev. Mod. Phys 1951;23:69.

91. Møller C, Plesset MS. Phys. Rev 1934;46:618.

92. Adamo C, Barone V. J. Chem. Phys. Lett 1997;274:242–250.

93. Becke AD. Phys. Rev. A 1988;38:3098–3100. [PubMed: 9900728]

94. Lee C, Yang W, Parr RG. Phys. Rev. B 1988;37:785–789.

95. Stephens PJ, Devlin FJ, Chabalowski CF, Frisch MJ. J. Phys. Chem 1994;98:11623–11627.

96. Hertwig RH, Koch W. Chem. Phys. Lett 1997;268:345–351.

97. Perdew JP, Burke K, Ernzerhof M. Phys. Rev. Lett 1996;77:3865–3868. [PubMed: 10062328]

98. Slater, JC. Quantum Theory of Molecular and Solids. Vol. 4: The Self-Consistent Field for Molecular and Solids. New York: McGraw-Hill; 1974.

99. Vosko SH, Wilk L, Nusair M. Canadian Journal of Physics 1980;58:1200–1211.

100. Perdew JP. Phys. Rev. B 1986;33:8822–8824.

101. Perdew JP, Wang Y. Phys. Rev. B 1992;45:13244–13249.

102. Perdew JP, Chevary Ja, Vosko SH, Jackson Ka, Pederson MR, Singh DJ, Fiolhais C. Physical Review B 1992;46:6671–6687.

103. Becke AD. J. Chem. Phys 1993;98:5648–5652.

104. Schmider HL, Becke AD. J. Chem. Phys 1998;108:9624–9631.

105. Voorhis TV, Scuseria GE. J. Chem. Phys 1998;109:400–410.

106. Becke AD. J. Chem. Phys 1996;104:1040–1046.

107. Adamo C, Barone VJ. J. Chem. Phys 1998;108:664–675.

108. Staroverov VN, Scuseria GE, Tao J, Perdew JP. J. Chem. Phys 2003;119:12129–12137.

109. Tao J, Perdew JP, Staroverov VN, Scuseria GE. Phys. Rev. Lett 2003;91:146401. [PubMed: 14611541]

110. Rey J, Savin A. Int. J. Quantum Chem 1998;69:581–590.

111. Krieger, JB.; Chen, J.; Iafrate, GJ.; Savin, A. Electron Correlations and Materials Properties. Gonis, A.; Kioussis, N., editors. New York: Plenum; 1999. p. 463

112. Toulouse J, Savin A, Adamo C. J. Chem. Phys 2002;117:10465–10473.

113. Zhao Y, Lynch BJ, Truhlar DG. J. Phys. Chem. A 2004;108:2715–2719.

114. Zhao Y, Lynch BJ, Truhlar DG. Phys. Chem. Chem. Phys 2005;7:43–52.

115. Gill PMW. Mol. Phys 1996;89:433–445.

116. Hamprecht FA, Cohen AJ, Tozer DJ, Handy NC. J. Chem. Phys 1998;109:6264–6271.

Figure 1.
Average unsigned bond length errors for GGA, hybrid-GGA, meta-GGA, and hybrid-meta-GGA functionals along with the Pople type basis sets.

Figure 2.
Average unsigned bond length errors for GGA, hybrid-GGA, meta-GGA, and hybrid-meta-GGA functionals along with the Dunning type basis sets.

Figure 3.
Average unsigned bond angle errors for GGA, hybrid-GGA, meta-GGA, and hybrid-meta-GGA functionals along with the Pople type basis sets.

Figure 4.
Average unsigned bond angle errors for GGA, hybrid-GGA, meta-GGA, and hybrid-meta-GGA functionals along with the Dunning type basis sets.

Figure 5.
Average unsigned vibrational frequency errors for GGA, hybrid-GGA, meta-GGA, and hybrid-meta-GGA functionals along with the Pople type basis sets.
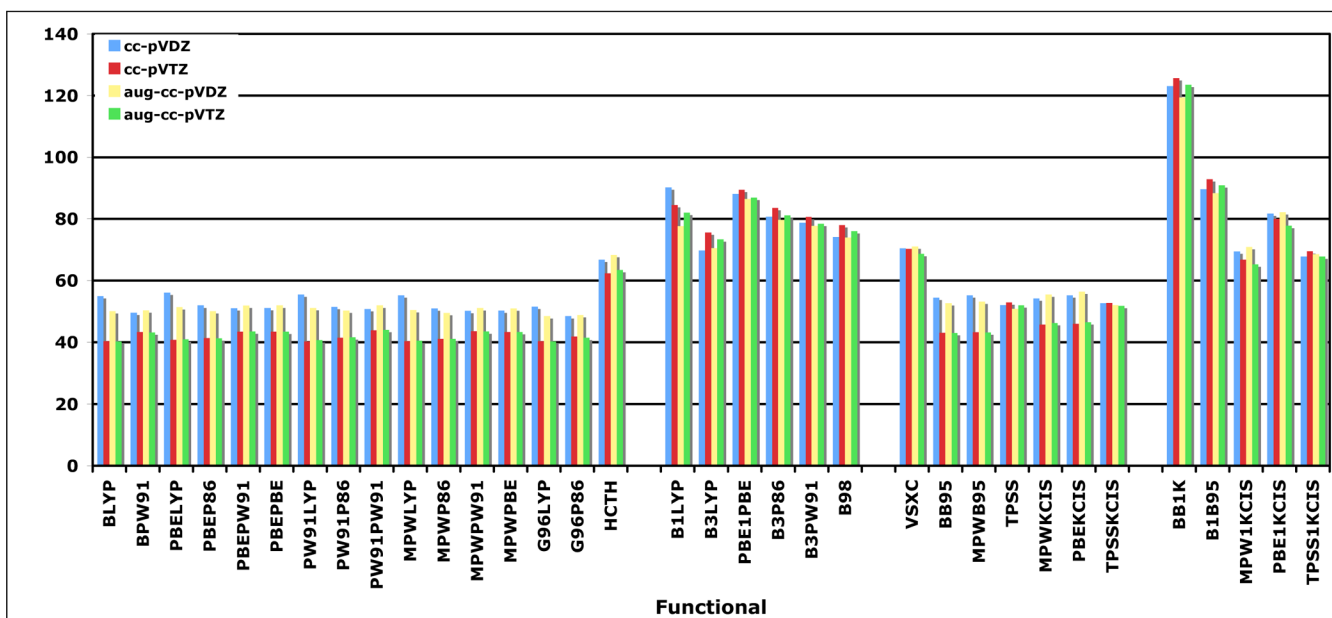
Figure 6.
Average unsigned vibrational frequency errors for GGA, hybrid-GGA, meta-GGA, and hybrid-meta-GGA functionals along with the Dunning type basis sets.
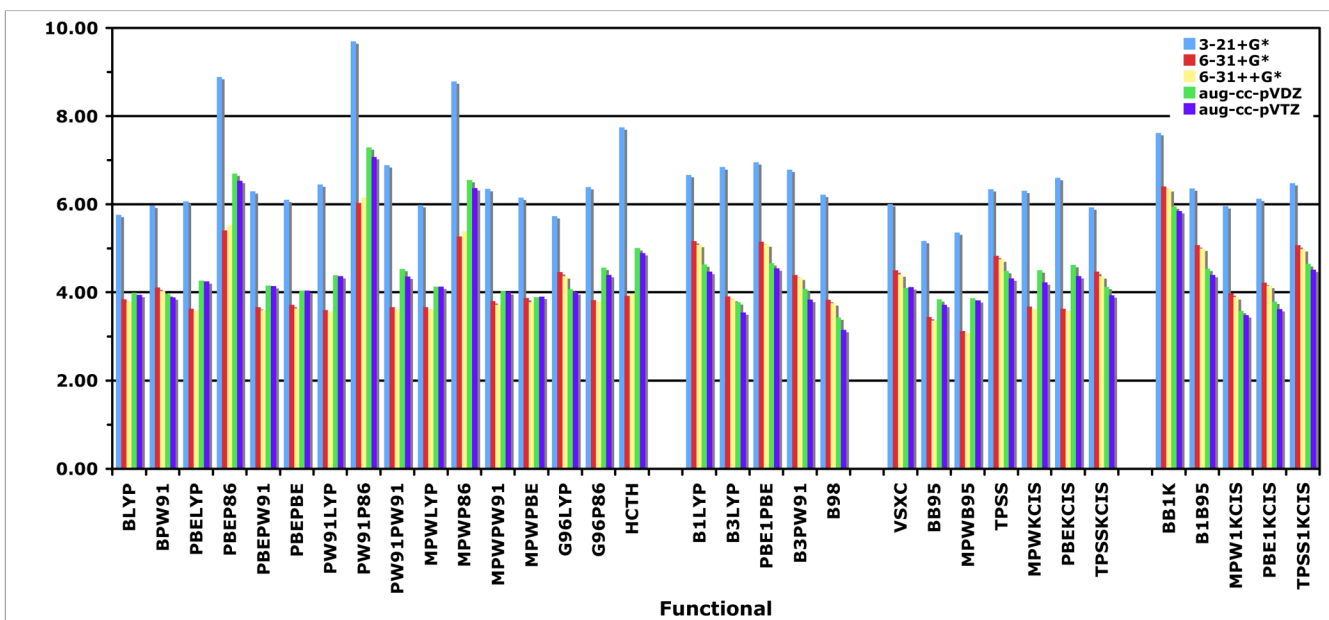
Figure 7.
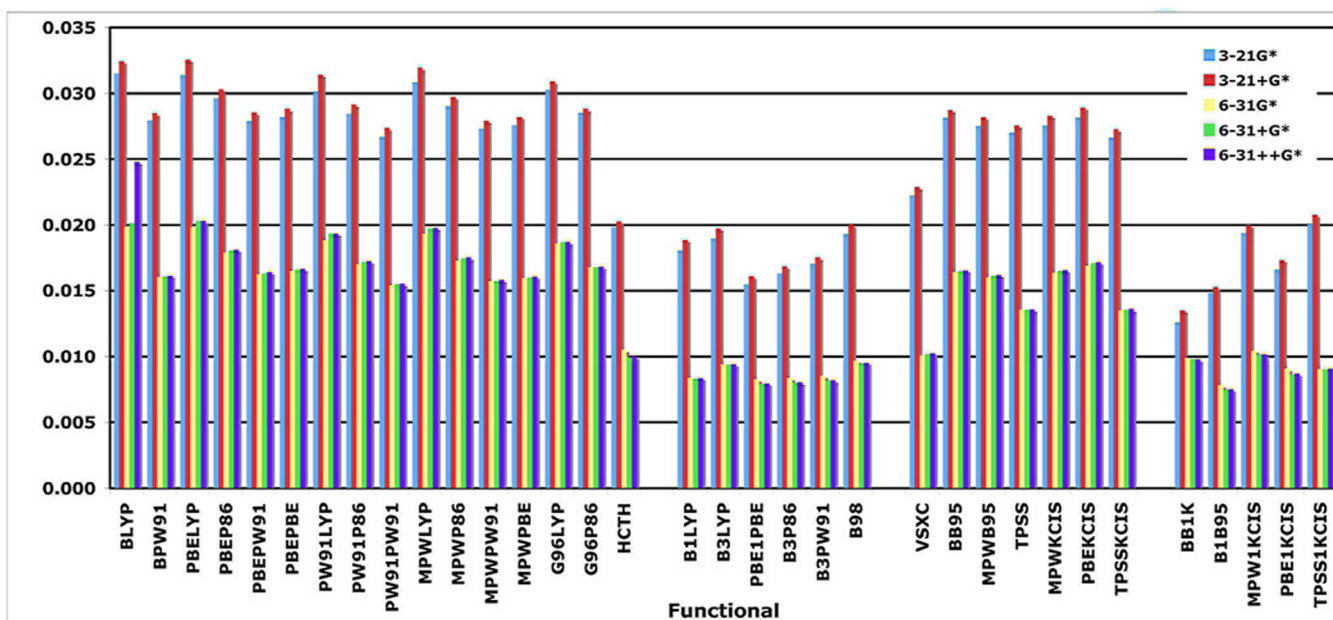Average unsigned electron affinity errors for GGA, hybrid-GGA, meta-GGA, and hybrid-meta-GGA functionals.
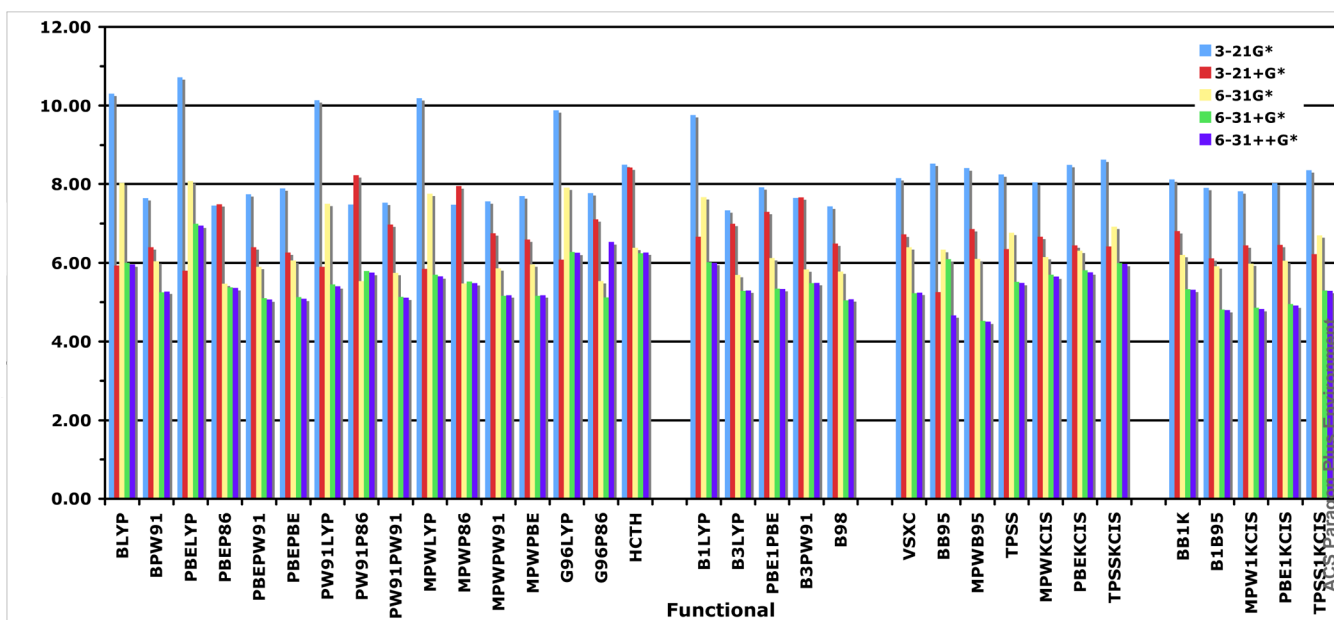
Figure 8.
Average unsigned ionization potential errors for GGA, hybrid-GGA, meta-GGA, and hybrid-meta-GGA functionals with Pople type basis sets.
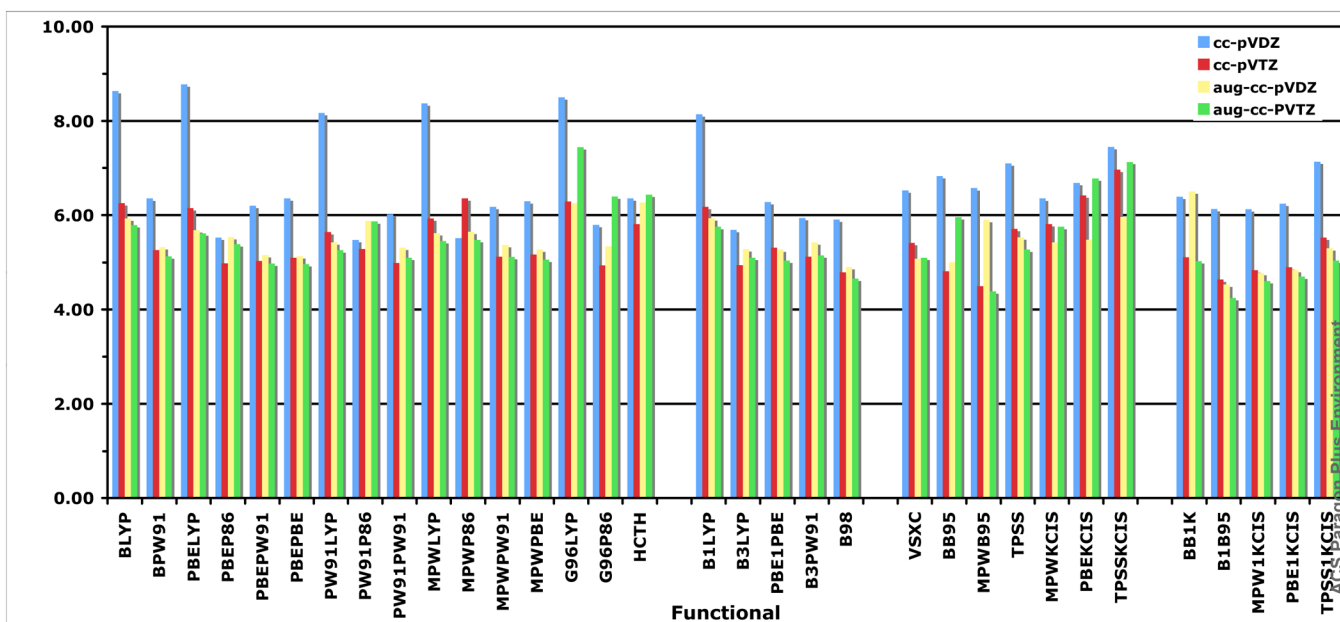
Figure 9.
Average unsigned ionization potential errors for GGA, hybrid-GGA, meta-GGA, and hybrid-meta-GGA functionals with Dunning type basis sets.
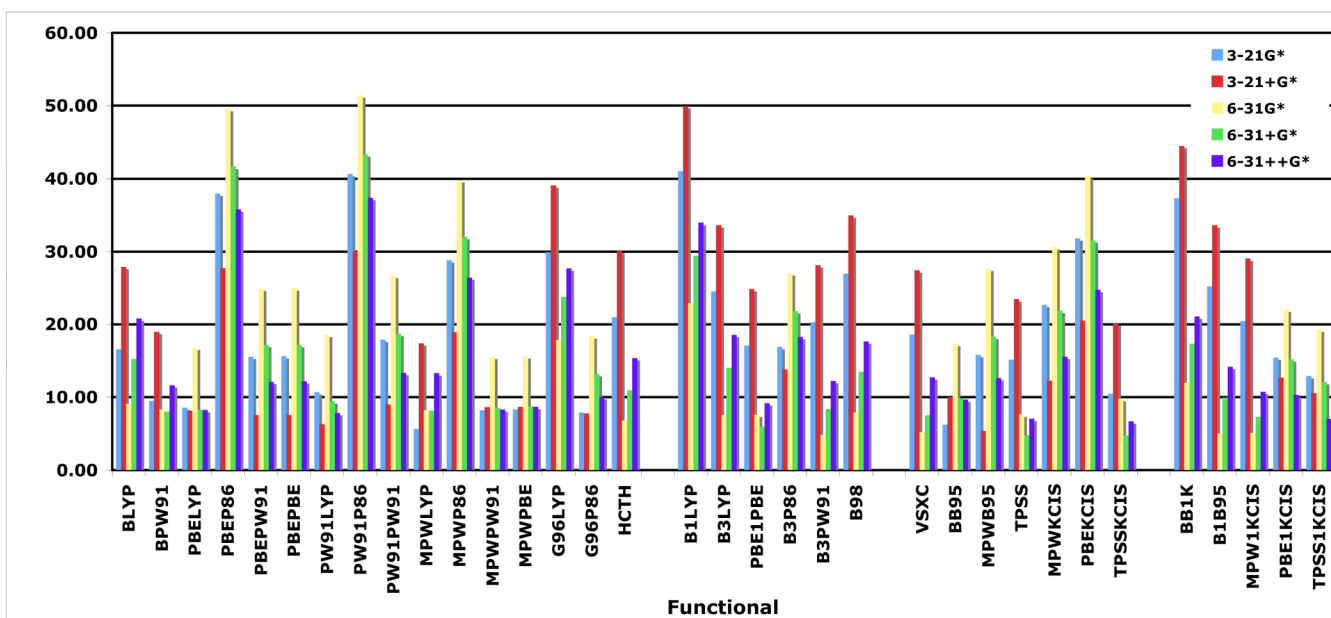
Figure 10.
Average unsigned heat of formation errors for the 5 Pople-style basis sets employed in this study.
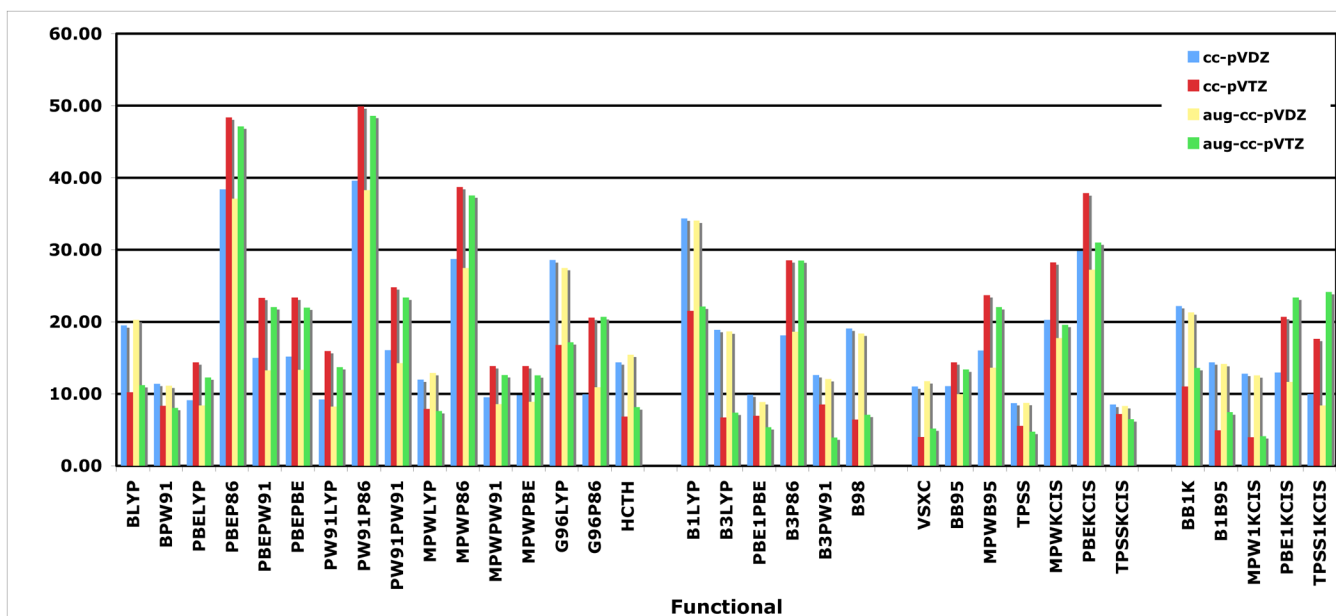
Figure 11.
Average unsigned heat of formation errors for the Dunning-type correlation-consistent basis functions used in this work.
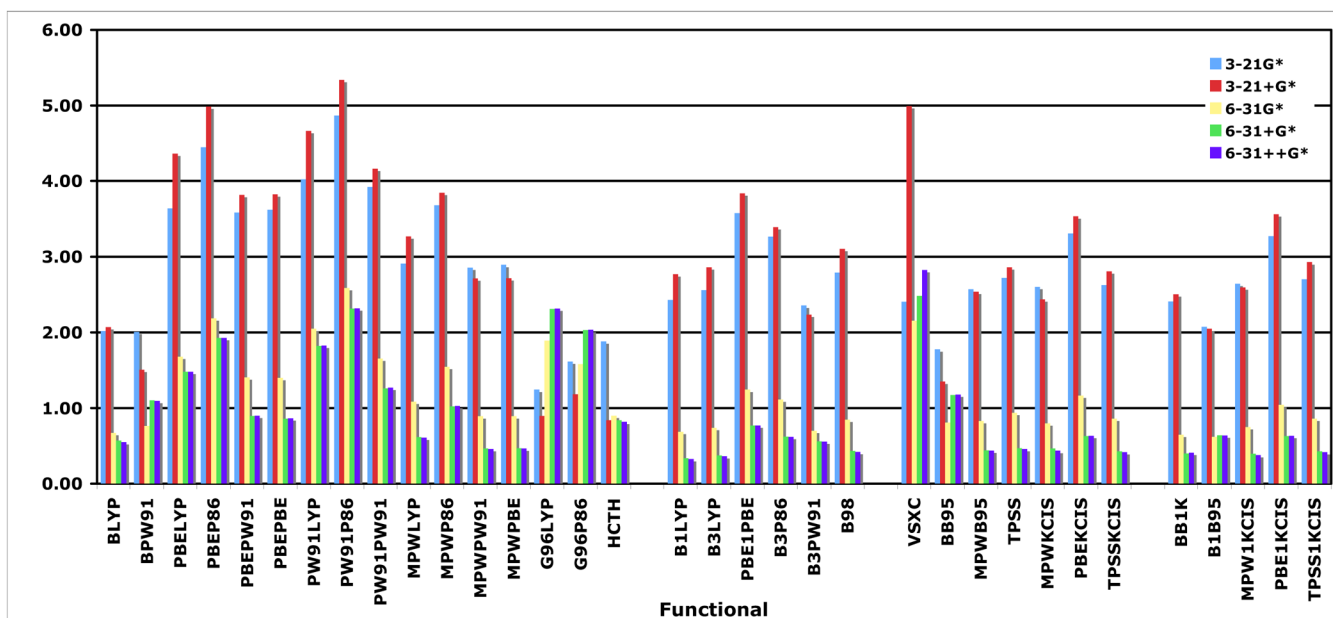
Figure 12.
Average unsigned hydrogen bond interaction energy errors for GGA, hybrid-GGA, meta-GGA, and hybrid-meta-GGA functionals along with Pople type basis sets.
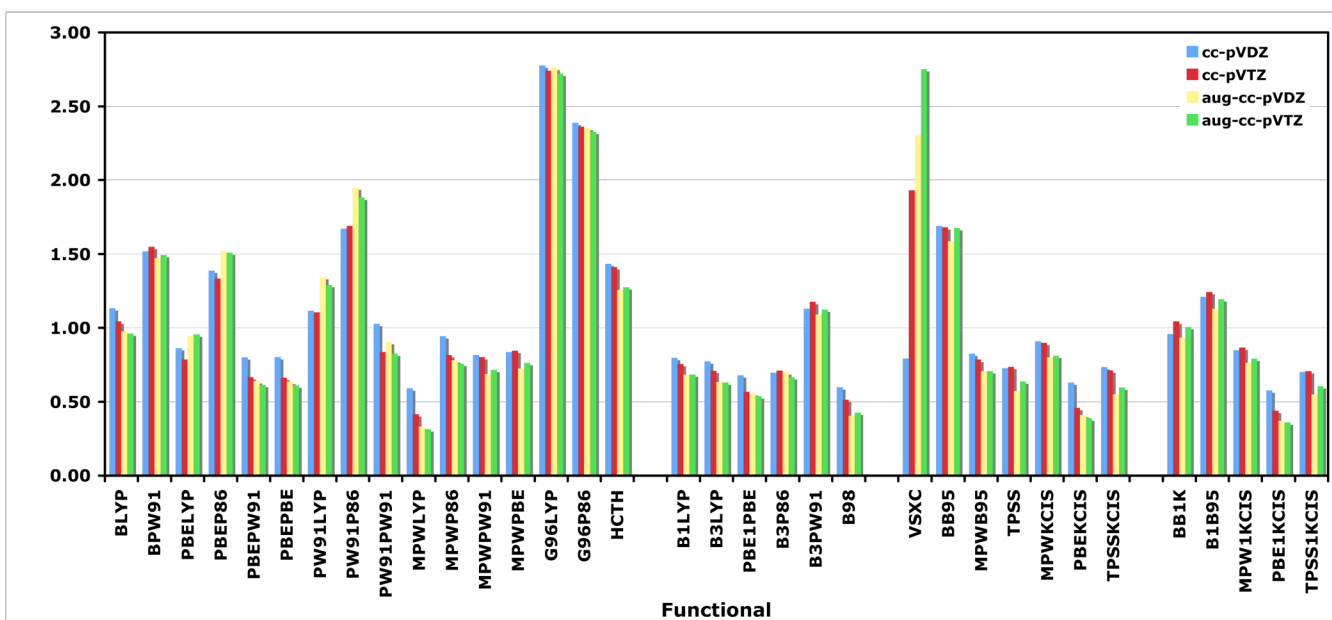
Figure 13.
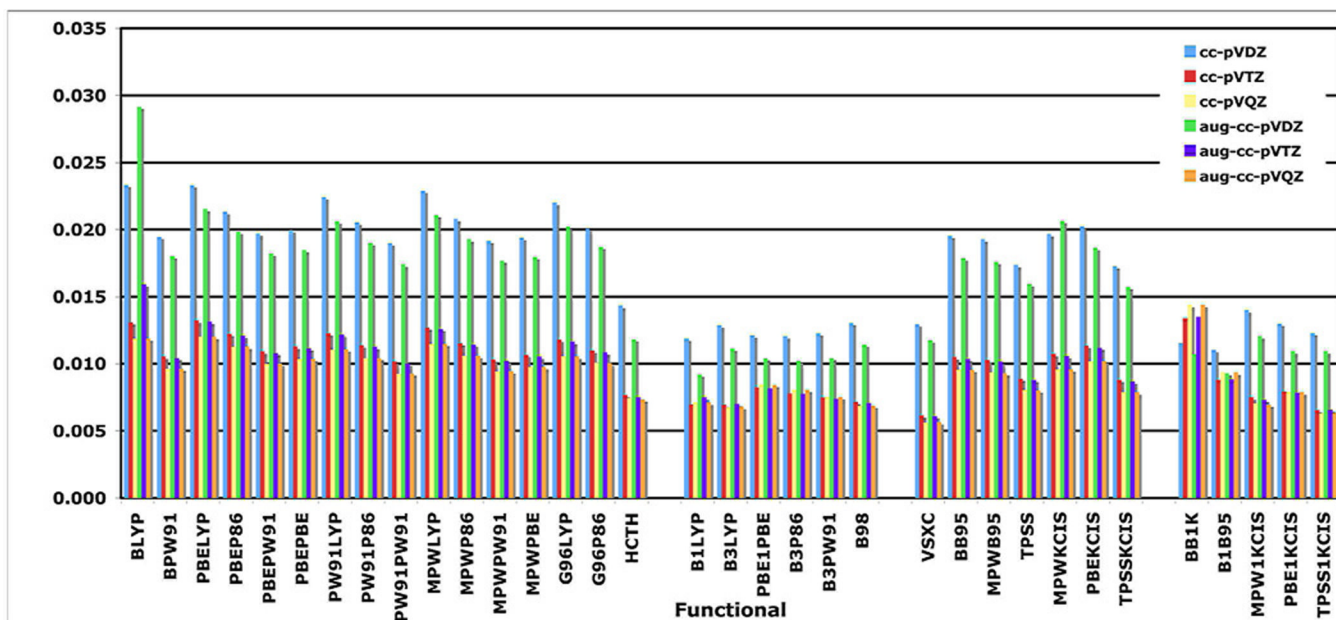Average unsigned hydrogen bond interaction energy errors for GGA, hybrid-GGA, meta-GGA, and hybrid-meta-GGA functionals along with Dunning type basis sets.
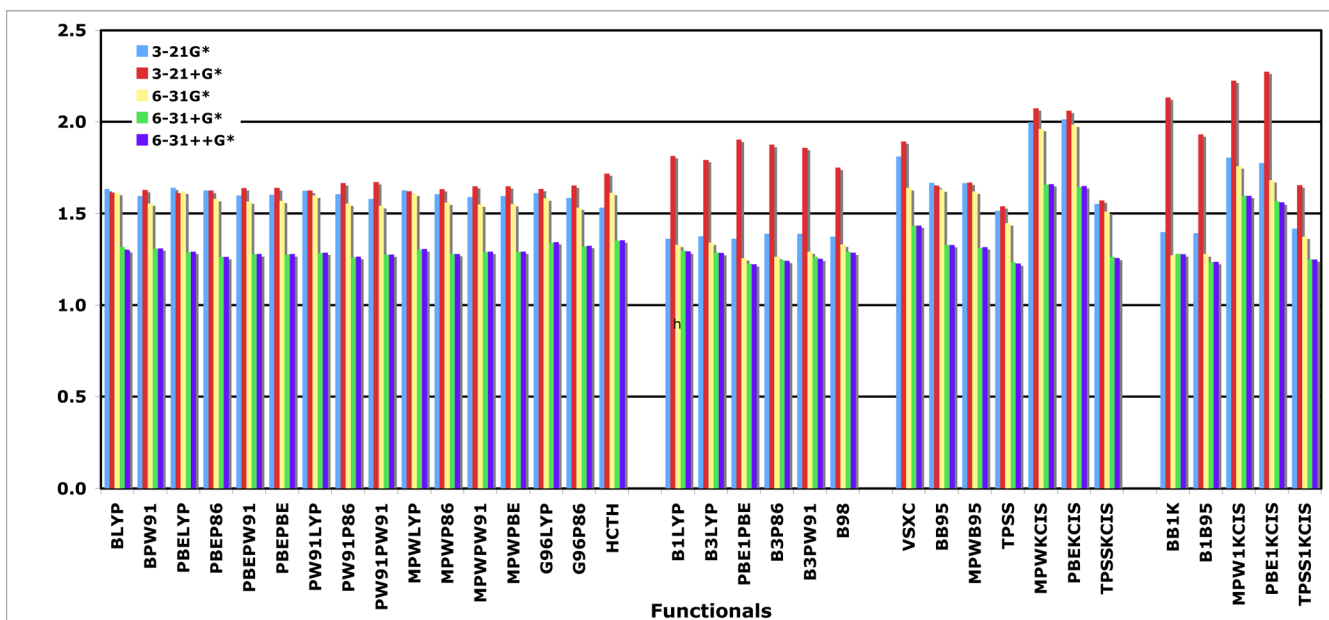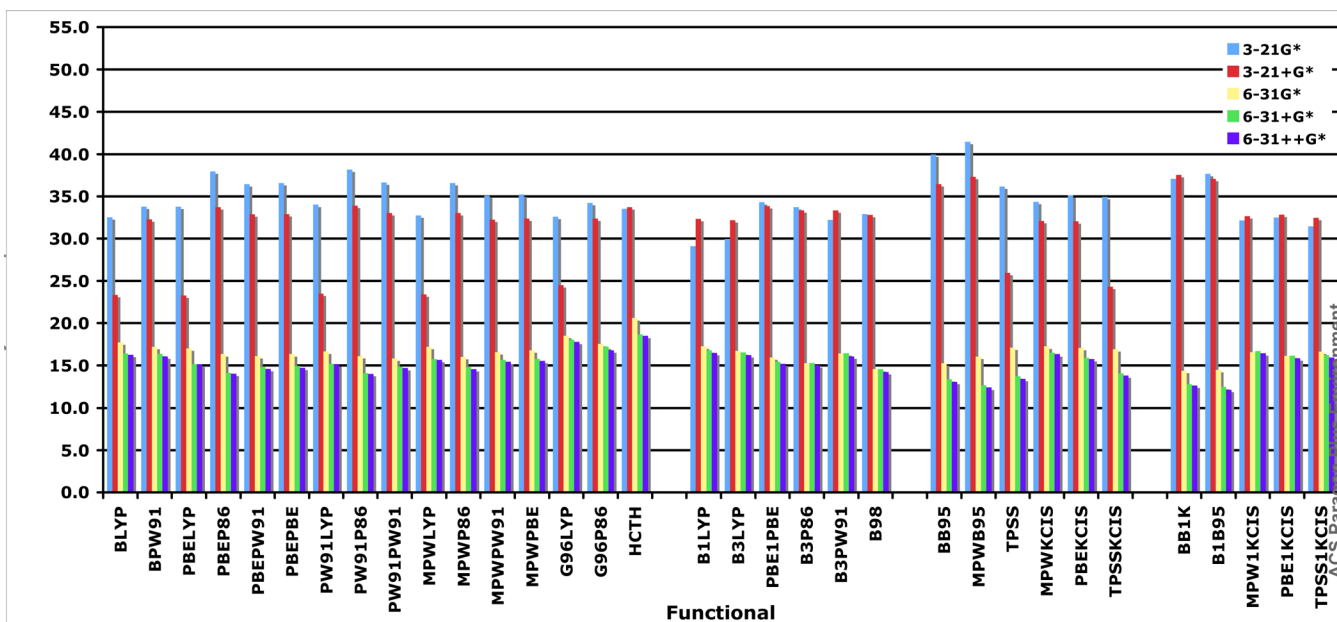
Figure 14.
Average unsigned conformational energy errors for GGA, hybrid-GGA, meta-GGA, and hybrid-meta-GGA functionals along with Pople type basis sets.
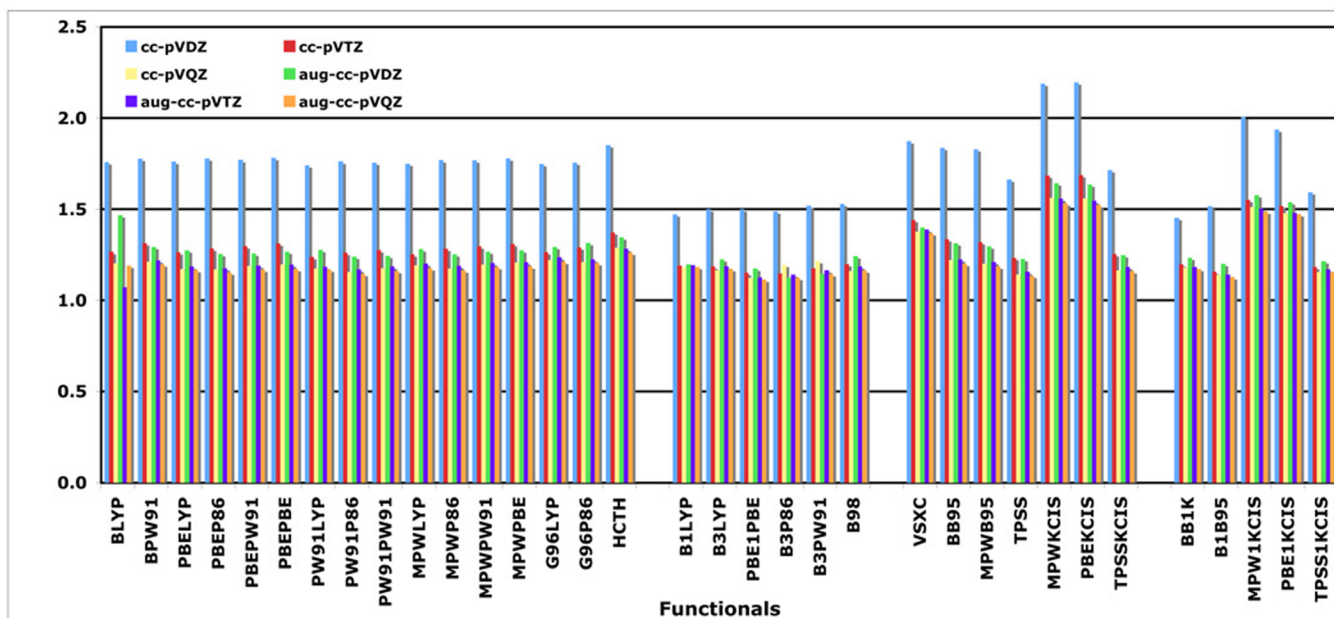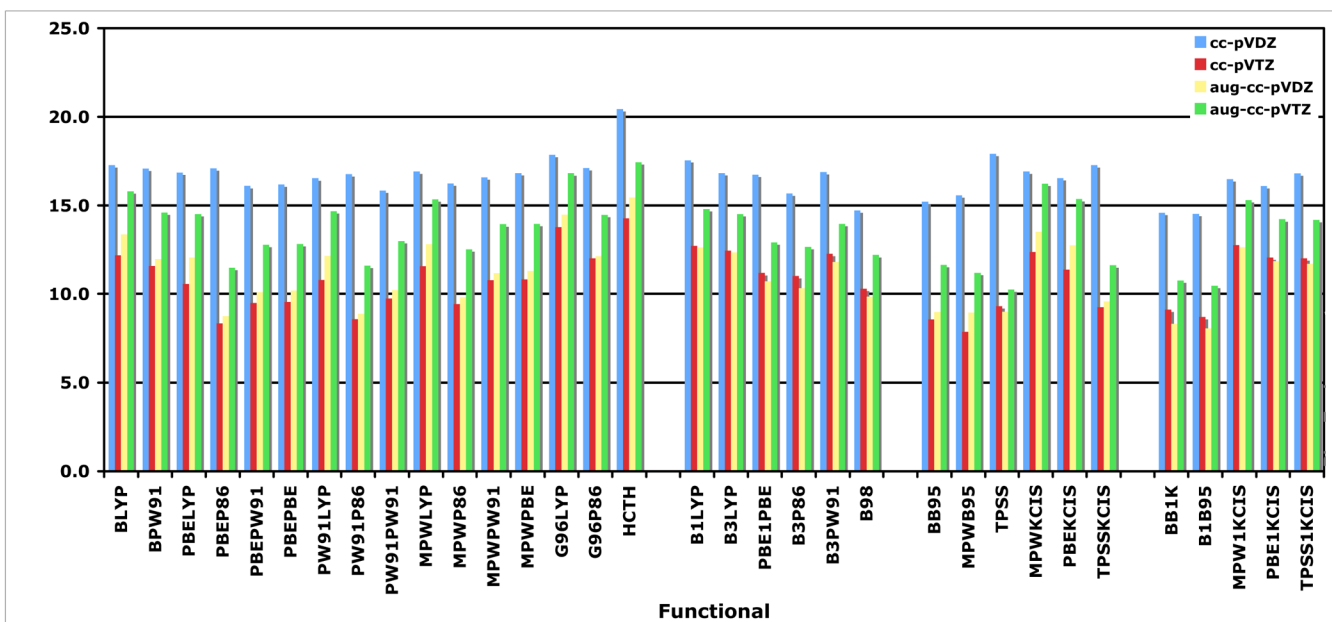
Figure 15.
Average unsigned conformational energy errors for GGA, hybrid-GGA, meta-GGA, and hybrid-meta-GGA functionals along with Dunning type basis sets.
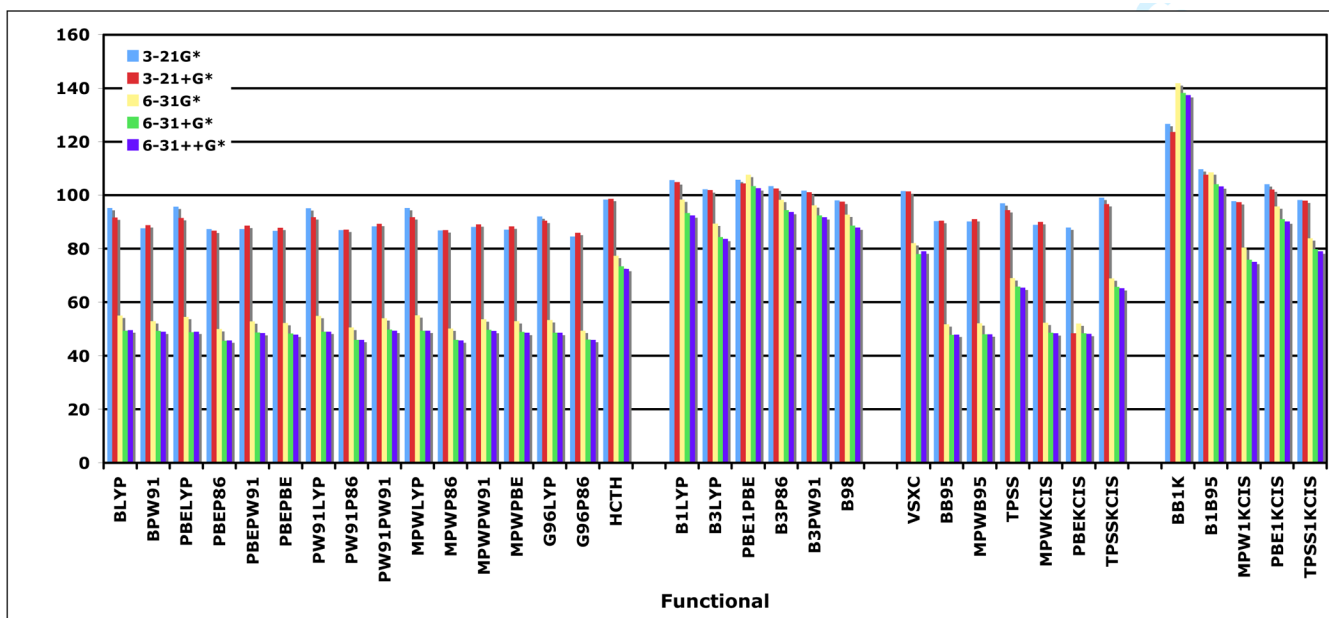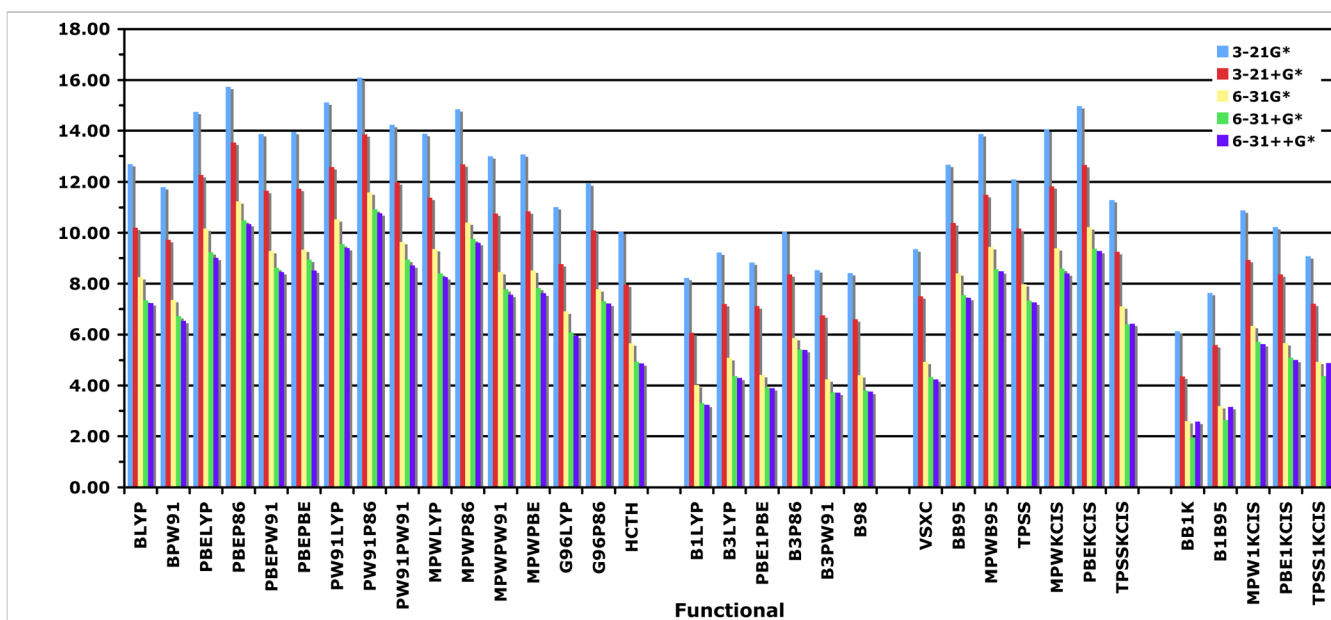
Figure 16.
Average unsigned barrier height energy errors for small radical transition state reactions along with the GGA, hybrid-GGA, meta-GGA, and hybrid-meta-GGA functionals along with Pople type basis sets.
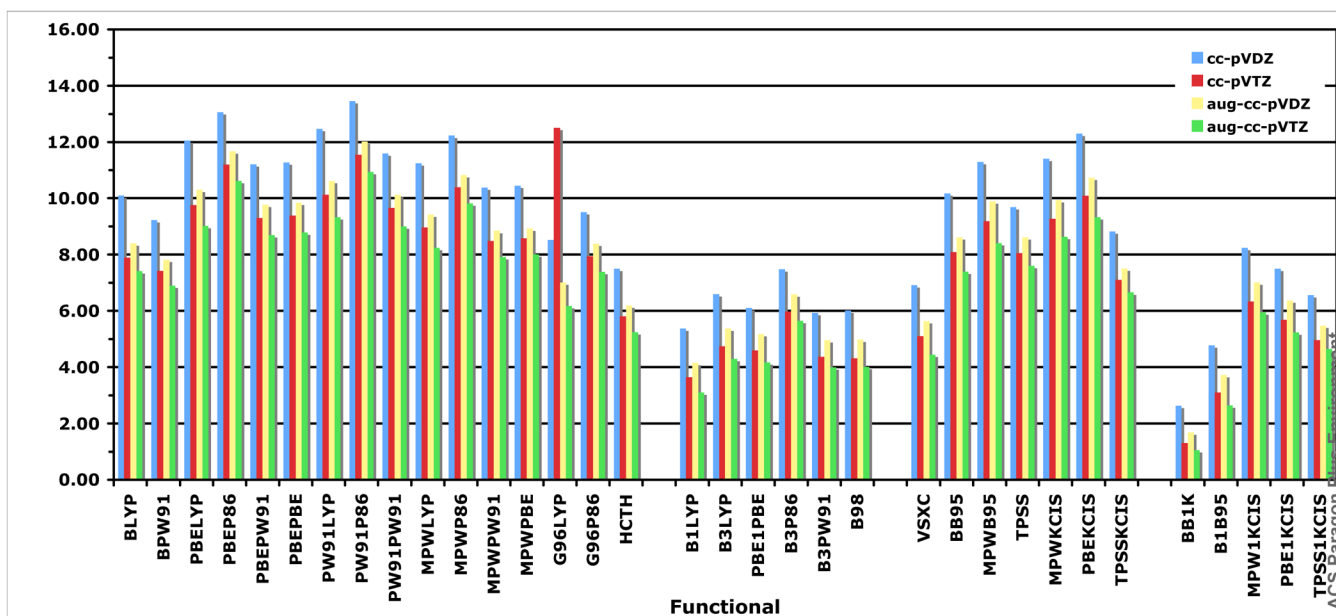
Figure 17.
Average unsigned barrier height energy errors for small radical transition state reactions along with the GGA, hybrid-GGA, meta-GGA, and hybrid-meta-GGA functionals along with Dunning type basis sets.
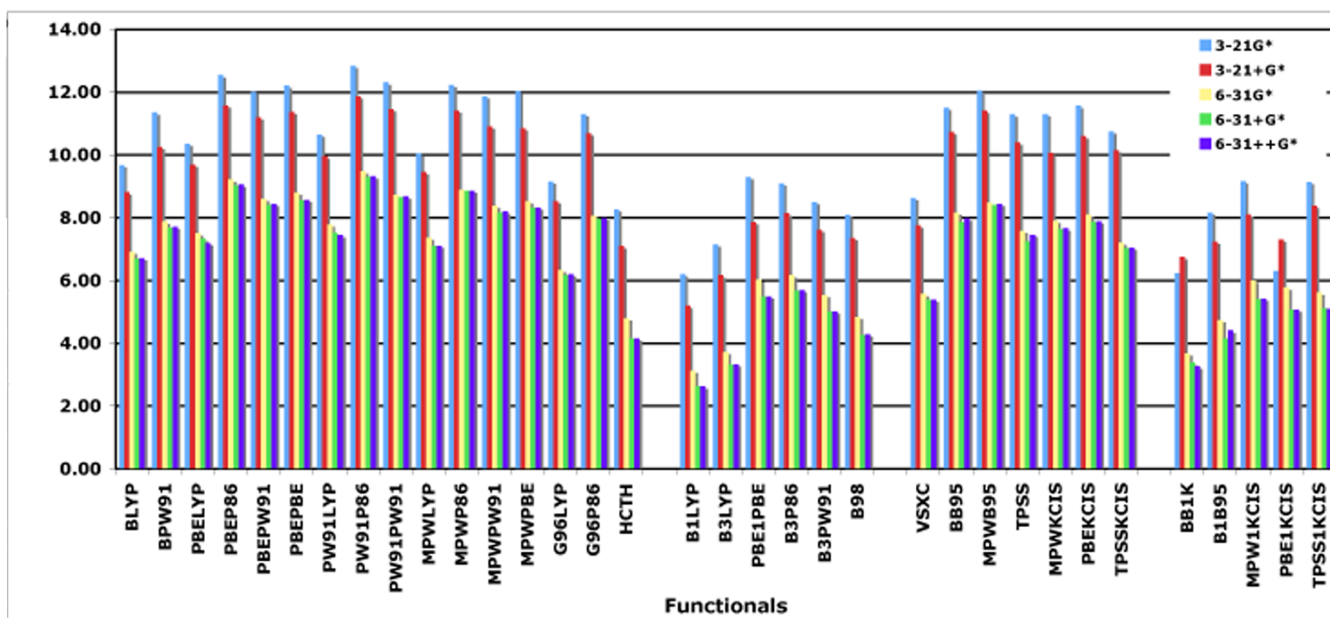
Figure 18.
Average unsigned barrier height energy errors for large singlet transition state reactions along with the GGA, hybrid-GGA, meta-GGA, and hybrid-meta-GGA functionals along with Pople type basis sets.
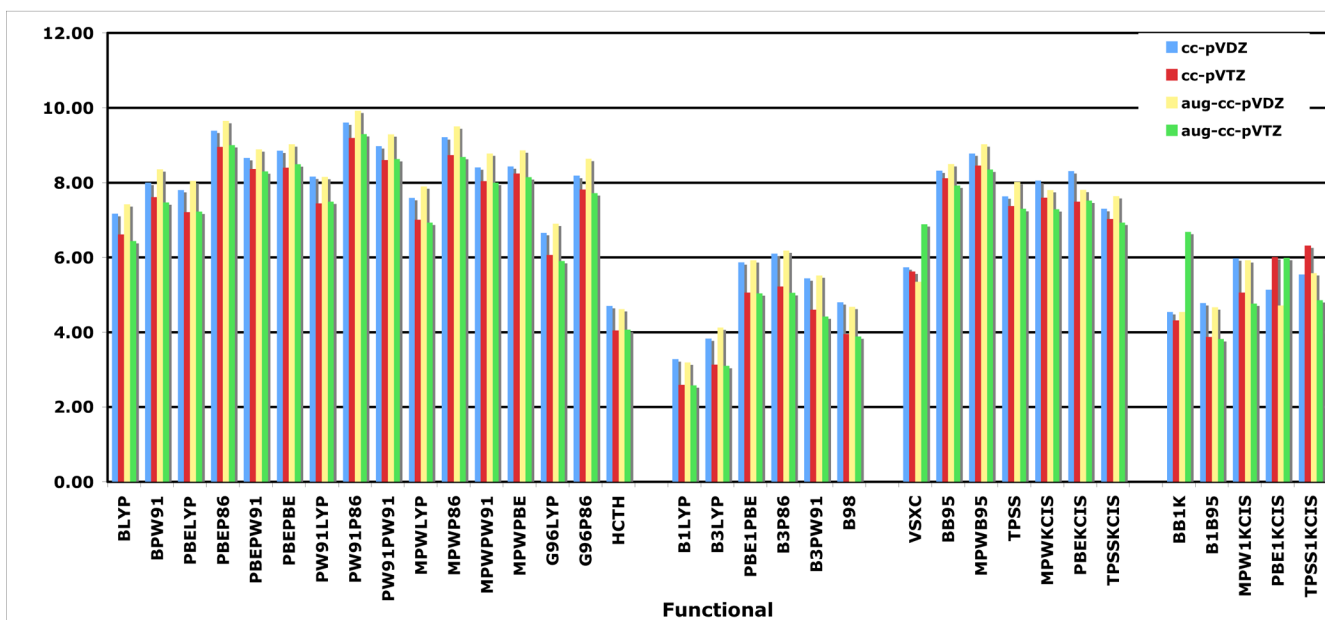
Figure 19.
Average unsigned barrier height energy errors for large singlet transition state reactions along with the GGA, hybrid-GGA, meta-GGA, and hybrid-meta-GGA functionals along with Dunning type basis sets.

Table 1

The 37 DFT methods and 2 wave function methods used in this work, with appropriate references.

Method	Reference	Method	Reference
HF	90	**hybrid-GGA**	
MP2	91	B1LYP	92–94
		B3LYP	93–96
		PBE1PBE	97
LSDA		B3P86	93,100
SVWN5	98, 99	B3PW91	93,101–103
SPL	98,101	B98	104
c-SVWN5(0.3)	53,98,99	**meta-GGA**	
GGA		VSXC	105
BLYP	93,94	BB95	93,106
BPW91	93,101,102	MPWB95	106,107
PBELYP	94,97	TPSS	108,109
PBEP86	97,100	MPWKCIS	106,110–112
PBEPW91	97,101,102	PBEKCIS	97,110–112
PBEPBE	97	TPSSKCIS	108–112
PW91LYP	94,101,102		
PW91P86	100–102	**hybrid-meta-GGA**	
PW91PW91	101,102	BB1K	93,106,113
MPWLYP	94,100,107	B1B95	93,106
MPWP86	100,107	TPSS1KCIS	108–112,114
MPWPW91	101,102,107	PBE1KCIS	73,97,110–112
MPWPBE	97,107	MPW1KCIS	78,92,106,110–112
G96LYP	94,115		
G96P86	100,115		
HCTH	116		

Table 2

Bond lengths, bond angles, and vibrational frequencies for HF, MP2, and LSDA methods.

Method	3-21G*	3-21+G*	6-31G*	6-31+G*	6-31++G*	cc-pVDZ	cc-pVTZ	cc-pVQZ	aug-cc-pVDZ	aug-cc-pVTZ	aug-cc-pVQZ
a) Bond Lengths (Å)											
HF	0.015	0.016	0.015	0.014	0.014	0.013	0.018	0.019	0.012	0.017	0.019
MP2	0.024	0.027	0.011	0.012	0.012	0.014	0.009		0.015	0.009	
SVWN5	0.024	0.024	0.018	0.017	0.017	0.021	0.014	0.014	0.019	0.014	0.014
SPL	0.025	0.025	0.018	0.017	0.017	0.022	0.014	0.014	0.019	0.014	0.014
c-SVWN5	0.034	0.035	0.025	0.025	0.025	0.029	0.019	0.018	0.027	0.019	0.018
b) Bond Angles (degrees)											
HF	1.85	2.45	1.45	1.55	1.54	1.40	1.50	1.51	1.48	1.53	1.53
MP2	1.55	2.02	1.31	1.39	1.37	1.65	1.22		1.26	1.17	
SVWN5	1.80	2.58	1.36	1.27	1.27	1.60	1.25	1.22	1.28	1.24	1.23
SPL	1.80	2.55	1.37	1.27	1.27	1.60	1.25	1.22	1.27	1.23	1.22
c-SVWN5	1.69	2.31	1.52	1.28	1.28	1.75	1.24	1.20	1.25	1.19	1.17
c) Vibrational Frequencies (cm^{-1})											
HF	210	203	236	235	234	211	209	203	207		
MP2	151	147	149	141	141	126	122	113	117		
SVWN5	83	87	51	50	50	58	51	59	52		
SPL	82	87	52	50	50	57	52	58	51		
c-SVWN5	93	100	58	57	58	75	63	71	65		

Table 3

Average unsigned electron affinity, ionization potential and heat of formation errors for HF, MP2, LSDA, and B3P86 methods.[a,b]

Electron Affinity

Method	3-21+G*	6-31+G*	6-31++G*	aug-cc-pVDZ	aug-cc-pVTZ	cc-pVDZ	cc-pVTZ	aug-cc-pVDZ	aug-cc-pVTZ
HF	26.40	29.05	28.95	28.90	29.63	26.33	25.74	25.19	25.40
MP2	11.14	10.73	10.62	5.81	4.70	11.44	9.78	6.74	5.53
SVWN5	9.37	6.25	6.36	7.58	7.53	7.68	8.33	8.59	8.75
SPL	9.92	6.79	6.90	8.14	8.04	7.46	8.42	8.70	8.83
c-SVWN5	12.04	14.80	14.65	13.60	13.68	23.37	19.85	19.06	18.69
B3P86	16.78	13.02	13.08	13.99	13.53	13.83	15.22	15.84	15.68

Ionization Potential

Method	3-21G*	3-21+G*	6-31G*	6-31+G*	6-31++G*	cc-pVDZ	cc-pVTZ	aug-cc-pVDZ	aug-cc-pVTZ
HF	26.53	23.00	25.70	24.74	24.76	26.33	25.74	25.19	25.40
MP2	15.59	9.77	10.45	10.42	5.84	11.44	9.78	6.74	5.53
SVWN5	10.74	10.29	7.57	8.52	8.48	7.68	8.33	8.59	8.75
SPL	10.50	10.37	7.49	8.62	8.57	7.46	8.42	8.70	8.83
c-SVWN5	24.93	17.31	22.57	19.08	19.05	23.37	19.85	19.06	18.69
B3P86	15.05	19.01	14.25	15.87	15.86	13.83	15.22	15.84	15.68

Heat of Formation

Method	3-21G*	3-21+G*	6-31G*	6-31+G*	6-31++G*	cc-pVDZ	cc-pVTZ	aug-cc-pVDZ	aug-cc-pVTZ
HF	289.94	294.01	252.94	256.28	258.10	261.27	248.30	259.40	248.49
MP2	58.23	55.95	83.74	84.53	83.27	96.10	135.06	122.98	133.85
SVWN5	125.83	127.57	135.97	128.06	121.78	124.24	135.06	122.98	133.85
SPL	128.66	117.21	143.48	133.70	127.46	129.90	144.22	128.62	139.49
c-SVWN5	13.45	9.44	19.47	26.46	27.14	19.48	29.44	18.95	18.10

[a] none values in kcal/mol.

[b] B3P86 for EA and IP only.

Table 4

Average unsigned hydrogen bond interaction energy, conformational energy, and reaction barrier height errors for HF, MP2, and LSDA methods.[a]

Hydrogen Bond Interaction Energy

Method	3-21G*	3-21+G*	6-31G*	6-31+G*	6-31++G*	cc-pVDZ	cc-pVTZ	aug-cc-pVDZ	aug-cc-pVTZ
HF	1.13	1.60	0.91	1.07	1.08	1.56	1.77	1.68	1.73
MP2	0.85	1.14	0.49	0.29	0.28	1.29	0.42	0.25	0.30
SVWN5	9.68	10.24	6.48	6.20	6.21	5.49	5.76	6.04	5.97
SPL	9.66	10.24	6.48	6.21	6.21	5.48	5.76	6.04	5.97
c-SVWN5	7.99	8.66	5.13	4.85	4.85	9.90	10.06	10.26	10.18

Conformational Energy

Method	3-21G*	3-21+G*	6-31G*	6-31+G*	6-31++G*	cc-pVDZ	cc-pVTZ	aug-cc-pVDZ	aug-cc-pVTZ
HF	27.6	38.7	24.2	22.1	22.2	27.7	20.3	22.0	21.0
MP2	30.8	21.7	18.8	16.8	15.5	19.8	7.4	6.8	8.9
SVWN5	51.9	39.1	19.5	15.6	15.4	17.1	9.9	8.8	11.6
SPL	52.1	39.3	19.7	15.6	15.5	17.4	10.1	8.9	11.6
c-SVWN5	51.2	34.4	17.4	17.0	17.0	17.8	10.2	10.0	15.6

Smnone Reaction Radical Barrier Height

Method	3-21G*	3-21+G*	6-31G*	6-31+G*	6-31++G*	cc-pVDZ	cc-pVTZ	aug-cc-pVDZ	aug-cc-pVTZ
HF	10.79	10.78	12.49	12.84	12.78	11.49	12.51	12.08	13.10
MP2	6.70	5.66	6.53	6.63	6.45	3.46	3.35	2.98	3.14
SVWN5	21.95	19.83	17.73	16.70	16.73	19.31	17.65	18.16	17.12
SPL	21.94	19.75	17.71	16.75	16.79	19.26	17.61	18.20	17.26
c-SVWN5	18.82	16.38	14.18	14.18	13.23	16.05	14.18	14.70	13.46

Large Reaction Singlet Barrier Height

Method	3-21G*	3-21+G*	6-31G*	6-31+G*	6-31++G*	cc-pVDZ	cc-pVTZ	aug-cc-pVDZ	aug-cc-pVTZ
HF	7.79	8.69	13.93	13.89	13.89	13.73	14.32	13.39	14.39
MP2	5.68	5.41	5.18	5.28	7.07	7.71	8.80		
SVWN5	19.86	17.81	12.61	12.04	12.08	12.01	11.83	12.54	12.21
SPL	19.82	17.78	12.59	12.02	12.05	11.99	11.75	12.49	11.83
c-SVWN5	14.11	13.25	13.01	11.31	11.35	11.22	11.93	11.74	12.33

[a] none values in kcal/mol.

Table 5

Rankings of functional/basis set combinations for none physical properties considered in this work. The first five functional/basis combinations include none basis sets, while the group of three functionals under each property shows the highest-ranking methods using the only Pople-type basis sets.

Rank Bond length		Avg. unsigned error error (Å)
1	VSXC/cc-pVQZ	0.0056
2	VSXC/aug-cc-pVQZ	0.0057
3	VSXC/aug-cc-pVTZ	0.0061
4	VSXC/cc-pVTZ	0.0061
5	TPSS1KCIS/cc-pVTZ	0.0063
1	B1B95/6-31+G*	0.0075
2	B1B95/6-31++G*	0.0075
3	B1B95/6-31G*	0.0078
Bond angle		**(deg)**
1	BLYP/aug-cc-pVTZ	1.07
2	PBE1PBE/aug-cc-pVQZ	1.11
3	B3P86/aug-cc-pVQZ	1.12
4	PBE1PBE/cc-pVQZ	1.12
5	B3P86/aug-cc-pVDZ	1.12
1	PBE1PBE/6-31++G*	1.22
2	PBE1PBE/6-31+G*	1.23
3	TPSSTPSS/6-31++G*	1.23
Frequencies		**(cm^{-1})**
1	G96LYP/aug-cc-pVTZ	40
2	PW91LYP/cc-pVTZ	40
3	BLYP/aug-cc-pVTZ	40
4	G96LYP/cc-pVTZ	40
5	MPWLYP/cc-pVTZ	40
1	PBEP86/6-31+G*	46
2	PBEP86/6-31++G*	46
3	MPWP86/6-31++G*	46
EA		**(kcal/mol)**
1	MPWB95/6-31++G*	3.08
2	MPWB95/6-31+G*	3.12
3	B98/aug-cc-pVTZ	3.15
4	BB95/6-31++G*	3.35
5	B98/aug-cc-pVDZ	3.42
1	MPWB95/6-31++G*	3.08
2	MPWB95/6-31+G*	3.12
3	BB95/6-31++G*	3.35
IP		**(kcal/mol)**
1	B1B95/aug-cc-pVTZ	4.25
2	MPWB95/aug-cc-pVTZ	4.38
3	MPWB95/cc-pVTZ	4.49
4	MPWB95/6-31++G*	4.50
5	MPWB95/6-31+G*	4.53
1	MPWB95/6-31++G*	4.50
2	MPWB95/6-31+G*	4.53
3	BB95/6-31++G*	4.67
HOF		**(kcal/mol)**
1	B3PW91/aug-cc-pVTZ	3.95
2	MPW1kcis/cc-pVTZ	3.97
3	VSXC/cc-pVTZ	3.99
4	MPW1KCIS/aug-cc-pVTZ	4.10
5	TPSSTPSS/aug-cc-pVTZ	4.73
1	TPSSKCIS/6-31+G*	4.76
2	TPSSTPSS/6-31+G*	4.77
3	B3PW91/6-31G*	4.79
Hydrogen Bond Interaction Energy		**(kcal/mol)**
1	MPWLYP/aug-cc-pVTZ	0.31
2	B1LYP/6-31++G*	0.33
3	MPWLYP/aug-cc-pVDZ	0.33
4	B1LYP/6-31+G*	0.34
5	PBE1KCIS/aug-cc-pVTZ	0.36
1	B1LYP/6-31++G*	0.33
2	B1LYP/6-31+G*	0.34
3	B3LYP/6-31++G*	0.36
Conformational Energy		**(% error)**
1	MPWB95/cc-pVTZ	7.90
2	B1B95/aug-cc-pVDZ	8.10
3	BB1K/aug-cc-pVDZ	8.30
4	PBEP86/cc-pVTZ	8.30

Rank		Avg. unsigned error error (Å)
Bond length		
5	BB95/cc-pVTZ	8.60
1	B1B95/6-31++G*	12.20
2	MPWB95/6-31++G*	12.40
3	B1B95/6-31+G*	12.50
SRBH		(kcal/mol)
1	BB1K/aug-cc-pVTZ	1.05
2	BB1K/cc-pVTZ	1.31
3	BB1K/aug-cc-pVDZ	1.69
4	BB1K/6-31+G*	1.95
5	BB1K/6-31++G*	2.58
1	BB1K/6-31+G*	1.95
2	BB1K/6-31++G*	2.58
3	BB1K/6-31G*	2.60
LSBH		(kcal/mol)
1	B1LYP/aug-cc-pVTZ	2.575
2	B1LYP/cc-pvTZ	2.591
3	B1LYP/6-31++G*	2.631
4	B1LYP/6-31+G*	2.637
5	B3LYP/aug-cc-pVTZ	3.102
1	B1LYP/6-31++G*	2.631
2	B1LYP/6-31+G*	2.637
3	B1LYP/6-31G*	3.123

Table 6

Average functional rankings and standard deviations for the "top fifteen" functionals along with 6-31+G* and aug-cc-pVDZ basis sets.

	6-31+G*	Avg. Rank	Std. Dev.
1	B1B95	10.7	11.9
2	B98	11.9	7.5
3	TPSSKCIS	13.6	8.4
4	TPSSTPSS	13.7	8.4
5	PBE1PBE	13.8	10.9
6	B3LYP	13.9	9.0
6	MPWB95	13.9	11.2
8	TPSS1KCIS	14.0	8.2
9	B3PW91	14.2	9.2
9	BB1K	14.2	12.4
11	MPW1KCIS	14.8	10.5
12	MPWPW91	15.8	5.6
13	PBEPW91	16.6	8.5
14	PBE1KCIS	16.7	9.2
15	MPWPBE	16.8	5.3
	aug-cc-pVDZ		
1	B98	10.1	8.8
2	B1B95	11.7	12.2
3	TPSS1KCIS	12.0	8.1
4	PBE1PBE	12.2	10.0
5	B3LYP	12.3	9.2
6	PBE1KCIS	12.8	10.9
7	TPSSTPSS	13.3	6.3
8	TPSSKCIS	13.6	7.6
9	B3PW91	13.8	9.0
10	MPWPW91	15.3	5.9
11	MPWPBE	15.7	6.7
12	MPW1KCIS	15.9	9.9
13	BB95	16.2	9.3
13	B1LYP	16.2	13.1
15	BB1K	16.7	13.8

Table 7

Performance of the "top fifteen" functionals along with the 6-31+G* basis set.

	HOF	IP	EA	H-bond	Freq	Length	Angle	Conf E	SRBH	LSBH
B1B95	9.94	4.81	5.07	0.64	104.1	0.0074	1.23	12.47	2.64	4.16
B98	13.47	5.05	3.83	0.43	88.6	0.0094	1.29	14.59	3.81	4.28
TPSSKCIS	4.76	5.99	4.47	0.43	65.6	0.0135	1.26	14.07	6.41	7.04
TPSSTPSS	4.77	5.52	4.83	0.47	65.8	0.0135	1.23	13.73	7.33	7.25
PBE1PBE	5.94	5.34	5.15	0.77	103.4	0.0079	1.23	15.45	3.92	5.49
B3LYP	14.03	5.29	3.91	0.38	84.4	0.0093	1.29	16.54	4.36	3.32
MPWB95	18.31	4.53	3.12	0.44	48.0	0.0161	1.31	12.66	8.57	8.41
TPSS1KCIS	12.06	5.30	5.07	0.43	79.8	0.0090	1.25	16.23	4.37	5.12
B3PW91	8.32	5.48	4.39	0.56	92.5	0.0081	1.26	16.46	3.73	5.01
BB1K	17.34	5.33	6.40	0.40	138.2	0.0098	1.28	12.79	1.95	3.38
MPW1KCIS	7.28	4.86	3.98	0.40	75.9	0.0101	1.60	16.71	5.71	5.41
MPWPW91	8.57	5.16	3.80	0.46	49.7	0.0157	1.29	15.67	7.78	8.17
PBEPW91	17.18	5.10	3.67	0.89	48.8	0.0163	1.28	14.84	8.62	8.41
PBE1KCIS	15.20	4.95	4.22	0.63	91.0	0.0086	1.57	16.18	5.09	5.07
MPWPBE	8.76	5.16	3.87	0.47	48.9	0.0159	1.29	15.79	7.83	8.32
Lowest Err.	TPSSKCIS	MPWB95	MPWB95	B1LYP	G96P86	B1B95	cSVWN5	B1B95	BB1K	B1LYP
Value	4.76	4.53	3.12	0.34	49	0.007	1.28	12.00	1.95	2.64
Highest Err.	SPL	cSVWN5	cSVWN5	SPL	BB1K	cSVWN5	VSXC	VSXC	SPL	SPL
Value	13.7	19.08	14.8	6.21	142	0.025	1.56	44	16.75	12.04
Avg. Err.	15.82	5.78	4.54	0.93	66.01	0.014	1.33	16.24	6.74	6.62

Notes: Errors given in the following units: bond length (Å), bond angle (degrees), frequency (cm^{-1}), ionization potential (kcal/mol), electron affinity (kcal/mol), heat of formation (kcal/mol), hydrogen-bond interaction energy (kcal/mol), conformational energy (percent error), reaction barrier height (kcal/mol). Average errors include none 37 density functionals considered in this work.

Table 8

Performance of the "top fifteen" functionals along with the aug-cc-pVDZ basis set.

	HOF	IP	EA	H-bond	Freq	Length	Angle	Conf E	SRBH	LSBH
B98	18.38	4.90	3.42	0.40	73.9	0.0114	1.24	9.85	4.98	4.68
B1B95	14.13	4.53	4.54	1.13	88.3	0.0093	1.20	8.06	3.72	4.67
TPSS1KCIS	8.35	5.30	4.64	0.55	68.5	0.0109	1.21	11.70	5.48	5.58
PBE1PBE	8.82	5.27	4.66	0.56	86.5	0.0104	1.17	10.71	5.17	5.92
B3LYP	18.66	5.28	3.78	0.63	70.5	0.0111	1.22	12.34	5.37	4.12
PBE1KCIS	11.63	4.84	3.79	0.37	82.2	0.0109	1.54	11.84	6.37	4.71
TPSSTPSS	8.72	5.53	4.49	0.57	50.9	0.0159	1.23	8.99	8.61	8.02
TPSSKCIS	8.31	5.96	4.13	0.55	52.1	0.0157	1.25	9.58	7.51	7.64
B3PW91	12.02	5.42	4.08	1.09	77.6	0.0104	1.15	11.80	4.96	5.52
MPWPW91	8.58	5.36	4.03	0.69	51.1	0.0177	1.27	11.17	8.85	8.77
MPWPBE	8.91	5.27	3.89	0.72	50.9	0.0180	1.27	11.29	8.92	8.85
MPW1KCIS	12.57	4.78	3.58	0.76	70.9	0.0121	1.58	12.64	7.00	5.92
BB95	9.94	5.00	3.85	1.58	52.6	0.0179	1.31	8.98	8.62	8.50
B1LYP	34.07	5.93	4.63	0.68	77.6	0.0092	1.20	12.61	4.15	3.19
BB1K	2.129	6.50	5.94	0.93	119.3	0.0107	1.23	8.31	1.69	4.54
Lowest Err.	PW91LYP	B1B95	B98	PBEKCIS	G96LYP	B1LYP	cSVWN5	B1B95	BB1K	B1LYP
Value	8.24	4.53	3.43	0.32	48	0.009	1.25	8.1	1.69	3.19
Highest Err.	SPL	cSVWN5	B3P86	cSVWN5	BB1K	BLYP	BLYP	VSXC	SPL	SPL
Value	128.62	19.06	13.99	10.26	119	0.029	1.6	51.5	18.2	12.54
Avg. Error	16.23	5.77	4.77	1.00	62.2	0.016	1.30	12.33	7.84	7.15

Notes: Errors given in the following units: bond length (Å), bond angle (degrees), frequency (cm^{-1}), ionization potential (kcal/mol), electron affinity (kcal/mol), heat of formation (kcal/mol), hydrogen-bond interaction energy (kcal/mol), conformational energy (percent error), reaction barrier height (kcal/mol). Average errors include none 37 density functionals considered in this work.